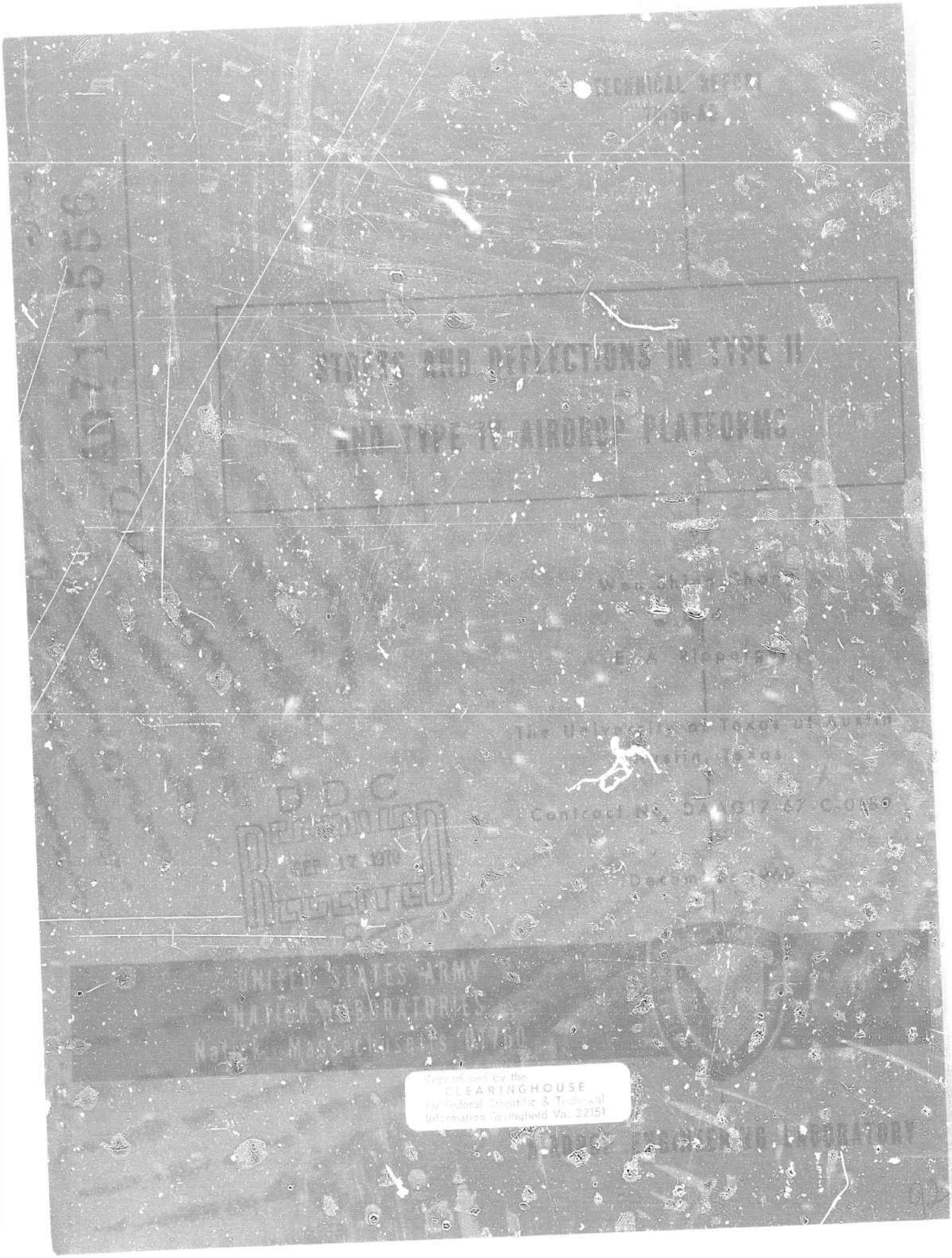
STEERS AND DEFLECTIONS IN STYPE II
AND TYPE IV AIRDROP PLATFORMS
RECEIVED
REPRODUCED
UNITED STATES ARMY
NATICK LABORATORIES
Natick, Massachusetts 01760
CLEARINGHOUSE
for Federal Scientific & Technical
Information Springfield Va. 22151
LABORATORY

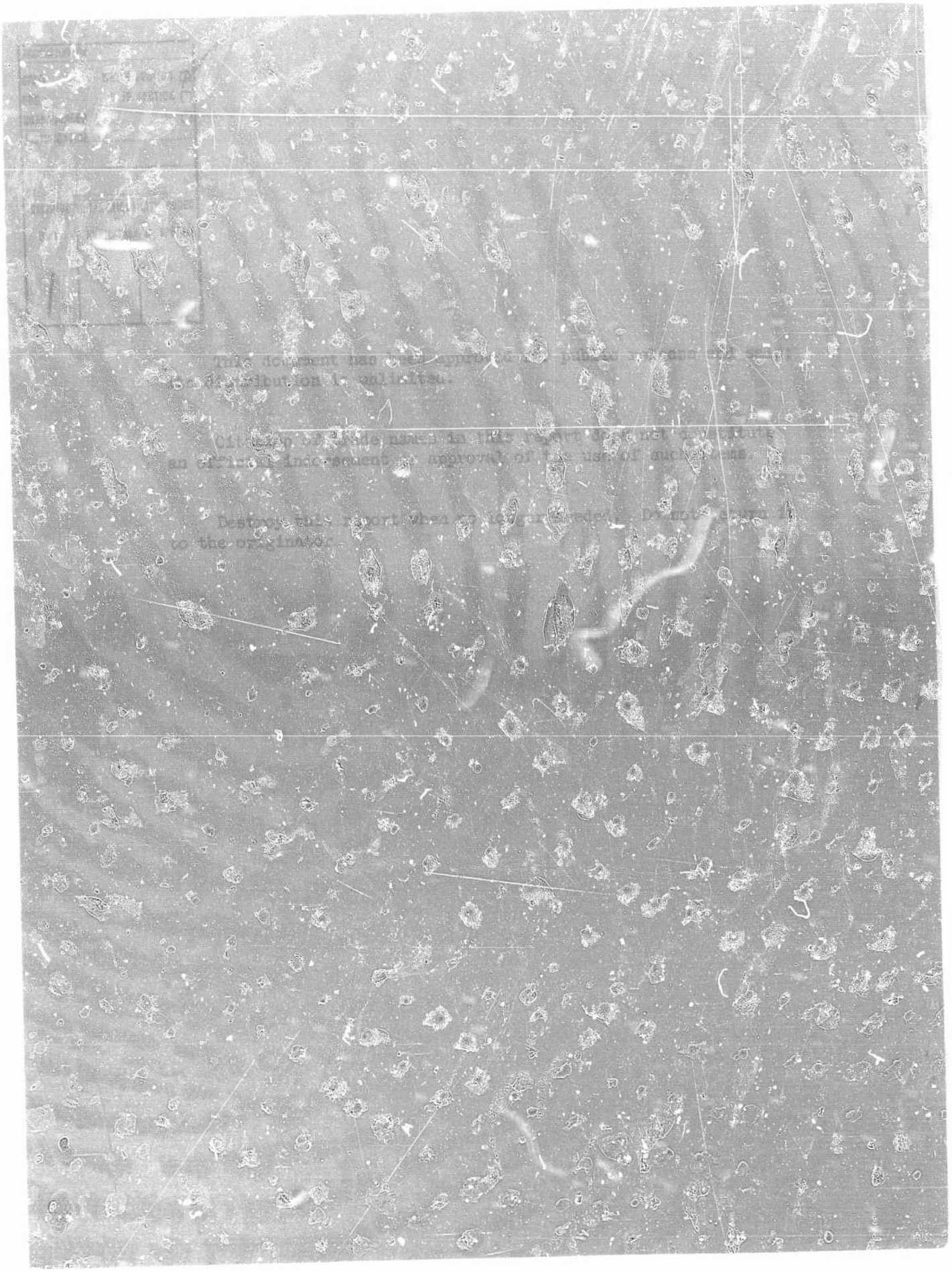

TECHNICAL REPORT

70-56-AD

STRESS AND DEFLECTIONS IN TYPE II AND TYPE IV AIRDROP PLATFORMS

by

Wen Shing Chang
E. A. Ripperger

Engineering Mechanics Research Laboratory
The University of Texas at Austin
Austin, Texas

Contract No. DAAG17-67-C-0189

Project reference:
1M121401 D195

December 1969

Airdrop Engineering Laboratory
U. S. ARMY NATICK LABORATORIES
Natick, Massachusetts 01760

Foreword

This work was performed during the period August 1967 through December 1969 under U.S. Army Natick Laboratories Contract No. DAAG-17-67-C-0189 for the Department of the Army project No. 1M121401D195 entitled "Exploratory Development of Airdrop Systems" Task 13- Impact Phenomena. The program is part of continuing investigation directed toward obtaining improved energy dissipater materials for airdrop landing mitigation and a better understanding of the response of airdroppable materiel to airdrop impact phenomena.

TABLE OF CONTENTS

	Page
List of Figures	iv
List of Symbols	vii
Abstract	ix
The Airdrop Procedure	1
Platform Description	1
Analysis	9
Static Loading	9
Formulation of the Problem	10
Experimental Technique and Results	12
Stiffness Properties of the Platforms	13
Further Static Loading Calculations	19
Type II Platform	19
Sign Convention	20
Type IV Platform	22
Dynamic Analysis	23
Principle	23
Type II Platform	24
Loading	24
Stiffness and Mass Matrices	25
Comparison of Displacement Calculations with 36 and 29 Degrees of Freedom	26
Summary	29
Conclusions	32
References	34
Appendices	
A - Typical Cross Sections	35
B - Tabulation of Deflections and Section Properties	50
C - Moments and Deflections for a Type II Platform	57
D - Computer Program for Analysis of Dynamic Response	67

LIST OF FIGURES

Figures		Page
1	The Airdrop Procedure	2
2	Parachute to Platform Connections	3
3	Forces in Four Suspension Slings During the Airdrop	4
4	Platform and Module Assembly Type II Modular Section	6
5	Type IV Platform and Module Assembly	7
6	Typical Platform Dimensions	8
7	Example of Grid Layout	9
8	Grid Element Displacements	10
9	Laboratory Loading Set-Up	14
10	Electrical Instrument Circuit	15
11	One Quarter Grid Layout of Type II Platform	16
12	One Quarter Grid Layout of Type IV Platform	17
13	Global Coordinates and Member Coordinates for Members AB and CD	20
14	Signs of the Moments and the Forces of Member AB	21
15	Signs of the Moments and the Forces of Member CD	21
16	Free Body Diagram for a Vertical Degree of Freedom	23
17	Displacements of Points 3 and 54 Calculated for 29 and 36 Degrees of Freedom	27

LIST OF FIGURES - Cont'd

Figures		Page
18 (a)	Displacement of Point 54 Relative to Point 3 with Sus. Sling RT. AFT Force of Fig. 3, Applied at Point 3	28
18 (b)	Applied Force Same as in (a) Except 0.45 Sec Taken as Starting Point for 29 Degrees of Freedom	28
19	Deflection Relative to Point 3 of Type II Platform Due to Dynamic Loads when Point 54 (Center) Reaches a Maximum	30
	APPENDIX A	
1A	Sections A - A and B - B of Type II Platform	36
2A	Section C - C of Type II Platform	37
3A	Section D - D of Type II Platform	38
4A	Section E - E of Type II Platform	39
5A	Section F - F of Type II Platform	40
6A	Section G - G of Type II Platform	41
7A	Taken Through Rail Slot of Type II Platform	42
8A	Section H - H of Type II Platform	43
9A	Section I - I of Type II Platform	44
10A	Section I - I of Type II Platform Taken Through Rail Slot	45
11A	Sections J - J and K - K of Type II Platform	46
12A	Sections L - L and M - M of Type II Platform	47
13A	Sections A - A and B - B of Type IV Platform	48
14A	Sections C - C and D - D of Type IV Platform	49

LIST OF FIGURES - Cont'd

Figures		Page
	APPENDIX C	
1C	Bending Moments and Deflections of Type II Platform with Support at Point 2	58
2C	Bending Moments and Deflections of Type II Platform with Support at Point 2	59
3C	Bending Moments and Deflections of Type II Platform with Support at Point 2	60
4C	Bending Moments and Deflections of Type II Platform with Support at Point 3	61
5C	Bending Moments and Deflections of Type II Platform with Support at Point 3	62
6C	Bending Moments and Deflections of Type II Platform with Support at Point 3	63
7C	Bending Moments and Deflections of Type II Platform with Support at Point 4	64
8C	Bending Moments and Deflections of Type II Platform with Support at Point 4	65
9C	Bending Moments and Deflections of Type II Platform with Support at Point 4	

LIST OF SYMBOLS

A = cross sectional area of a member

a_{ij} = element of stiffness matrix for a member

BM = bending moment

b = width or length of a member cross section

c = distance from centroid of the cross section to the extreme fiber

d = distance from the reference axis of each element to the reference axis of the whole cross section

E = modulus of elasticity

F_i = external force corresponding to the i^{th} degree of freedom

g = acceleration of gravity

I = moment of inertia for a member

K = torsional constant or stiffness of the system

K_{ij} = element of stiffness matrix of the system

M = bending moment, same as BM

M_i = mass or mass moment of inertia of the i^{th} degree of freedom

m_i = factor used in Runge-Kutta-Gill integration method

N = number of total degrees of freedom

P_i = force or moment applied to the i^{th} degree of freedom of the system

p_i = force or moment applied to the i^{th} degree of freedom of a member

R_i = resistance at the i^{th} degree of freedom due to the stiffness of the system

LIST OF SYMBOLS
(Cont'd)

TM = torsion

t = thickness of a member cross section, or time

U = strain energy of the system

U_i = static displacement in the i^{th} degree of freedom of the system

u_i = static displacement in the i^{th} degree of freedom of a member

V = shear

v = velocity

X_i = global coordinates

y_i = dynamic displacement of the i^{th} degree of freedom of the system

ε_i = member coordinates

σ = bending stress

ν = Poisson's ratio

ABSTRACT

Severe stress conditions may develop during the extraction and parachute deployment phases of an air drop with a stressed platform. The platform stresses and deflections during that dynamic loading period are computed by treating the platform as a planar network of beams rigidly connected at the joints. Stiffness properties of the beams in the network are calculated approximately using standard methods and then refined to more exact values by comparing measured deflections under static loading to computed deflections. These stiffness properties are then used in the analysis of the dynamic loading. Equations of motion are written for each degree of freedom using a lumped mass representation for the loads. Deflections at the joints of the network are obtained by solving the equations of motion using the Runge-Kutta-Gill numerical procedure. Stresses are then determined from the deflections. It is found that the maximum deflection at the center of a 3 module, Type II platform loaded with a total load of 9000 lb. distributed over the central portion of the platform is 5.17 in. dynamically, as compared to 1.89 in. for static loading. The maximum stress at the center of the platform is 24,500 psi for the dynamic loading as compared to 6230 psi for static loading. Similar results for the Type IV platform are not available. Also, dynamic stresses in the side rails have not been computed.

STRESS AND DEFLECTIONS IN TYPE II AND TYPE IV AIRDROP PLATFORMS

1. The Airdrop Procedure

In the usual procedure for making an airdrop the platform which carries the load is initially supported in the aircraft on rollers. When the drop begins a small extraction parachute which is attached to the end of the platform is deployed. This parachute pulls the platform with its load out of the aircraft in a horizontal attitude (see Fig. 1, step 1). When the platform is clear of the aircraft the extraction parachute releases and deploys the main parachute (Fig. 1, step 2). As the main parachute fills and retards the motion of the platform a dynamic load is developed (Fig. 1, step 3). The platform deflections and stresses which result from this load are the subject of this study.

The platform is suspended from the parachute by four slings, one attached at each corner. These slings are attached to a common point, as shown in Fig. 2, at the lower end of the parachute shrouds.

The maximum deceleration phase of the drop while the main parachutes are filling lasts for approximately two seconds. Some typical values of the tensions in each of the four slings during the initial phase of an airdrop are shown in Fig. 3. This set of measurements identified as Drop 0050F, 17 Jan. 67 was supplied by the U.S. Army Natick Laboratories.

There are three principal parameters involved in the calculations of the stresses and deflections in the platform. These parameters are (1) The mass, including the mass of the platform itself and the load on the platform; (2) Platform stiffness; and (3) The deceleration of the platform. This parameter is introduced into the calculations by using the measured forces in the slings.

2. Platform Description

Two principal types of airdrop platforms are considered here. These are: (1) The Type II platform. This platform is made up of modules which are approximately nine feet wide and four feet long. The modules consist of a balsa wood core with a thin aluminum skin on the top and bottom, a channel section stiffener along the long edges and a box section stiffener along the short edges. (2) The Type IV platform. This platform is made up of modules which consist of 2 in. x 6 in. wood stringers sandwiched between 1/2 in. plywood sheets.

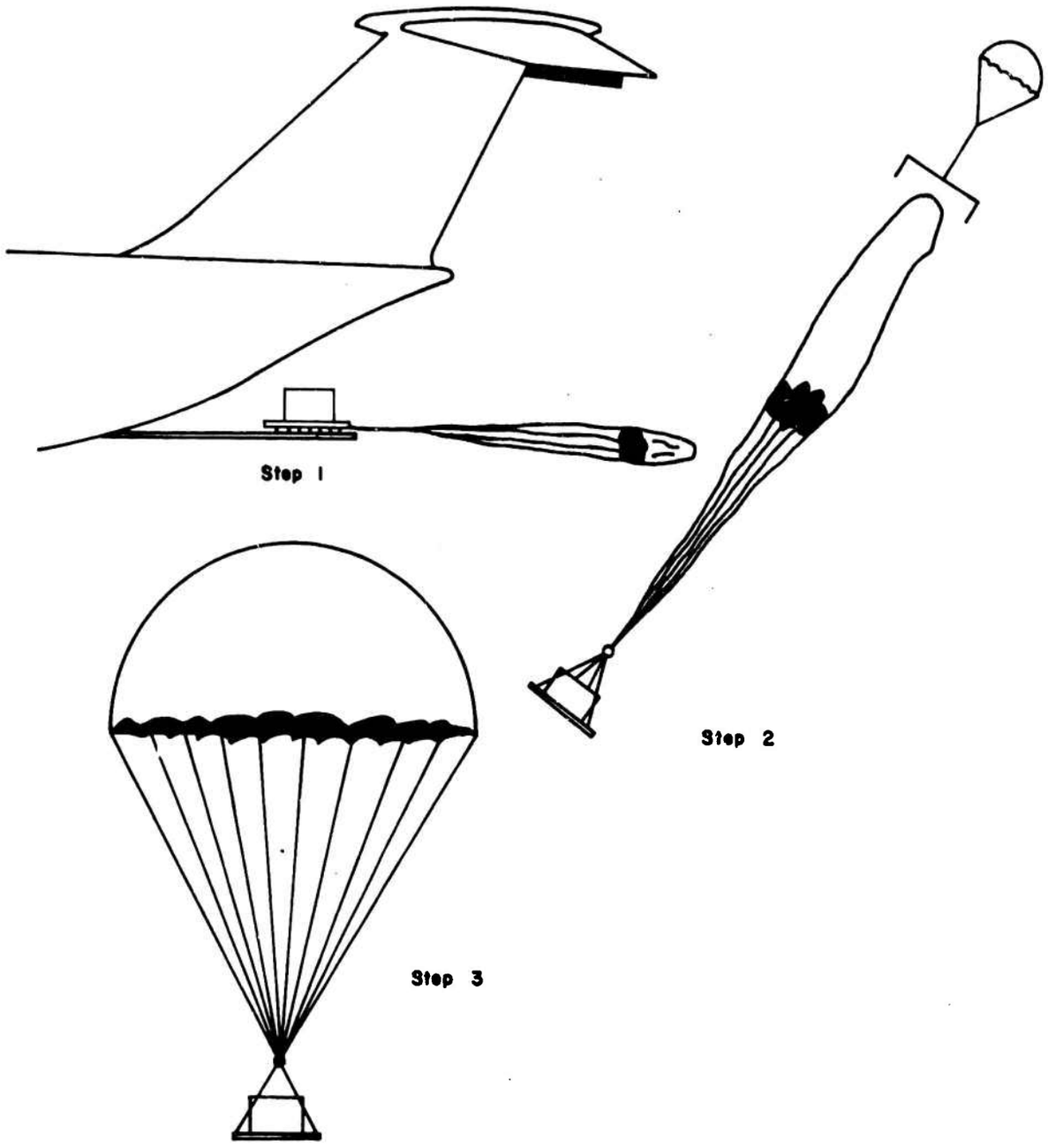

Fig. 1 The Airdrop Procedure

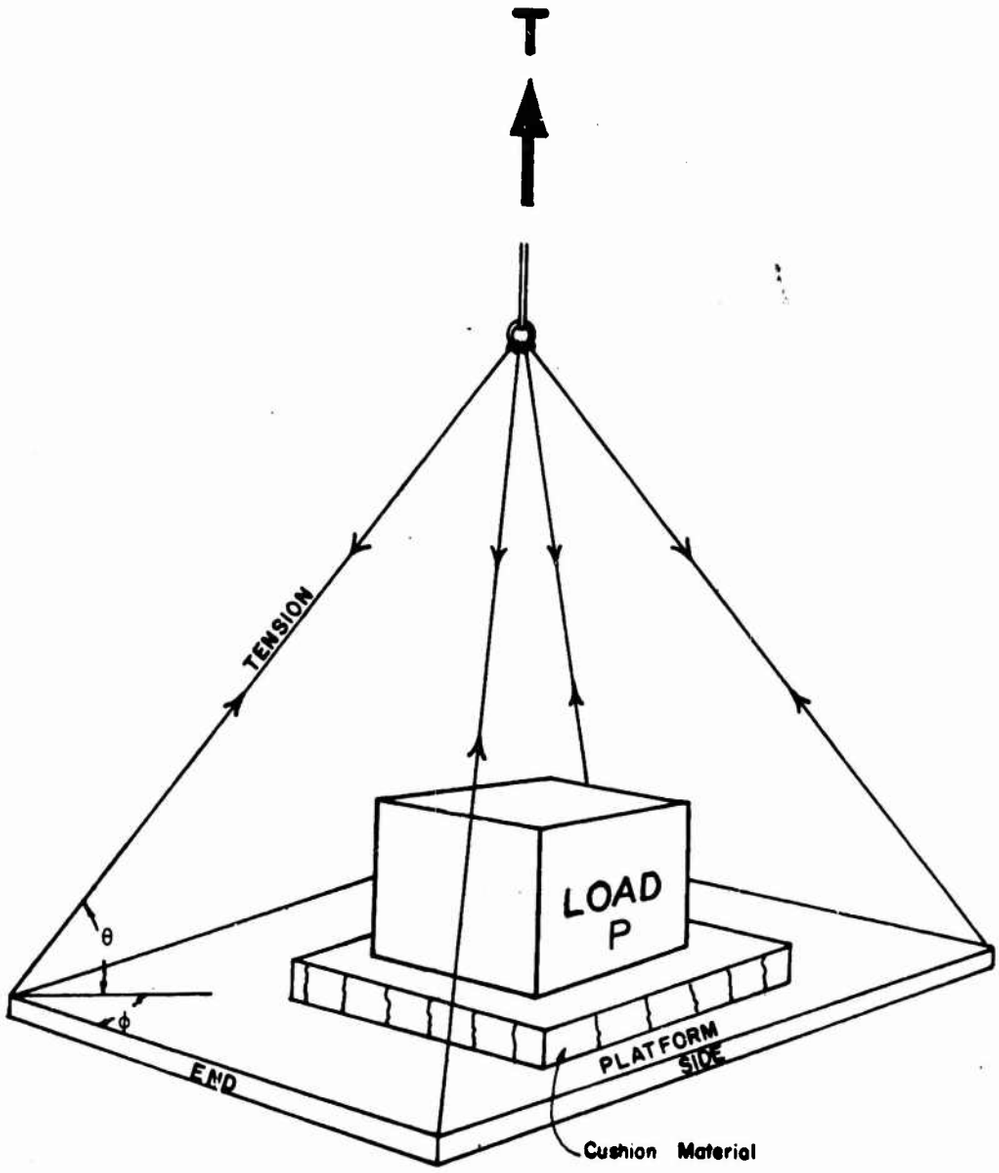

Fig. 2 Parachute to Platform Connections.

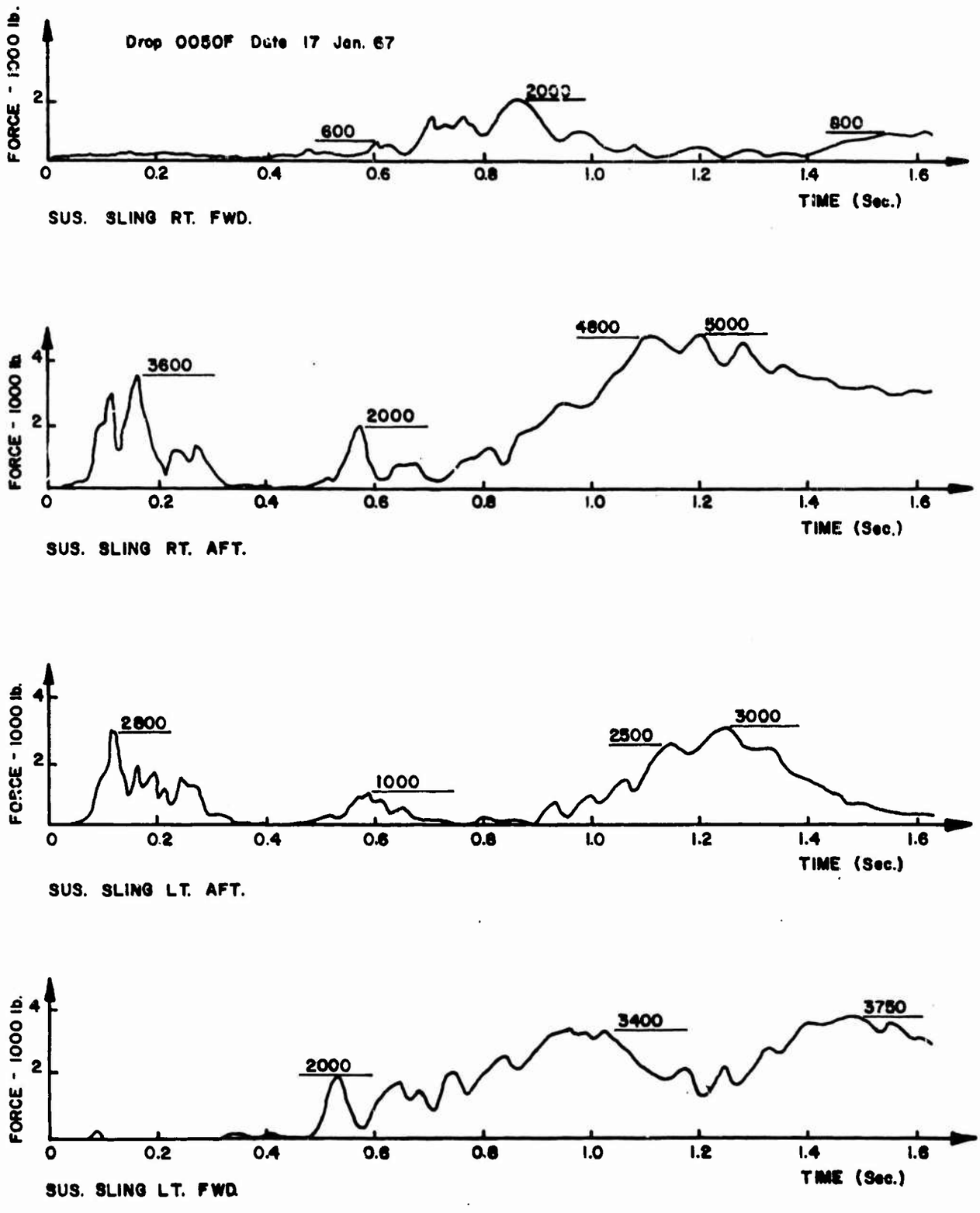

Fig. 3 Forces in Four Suspension Slings During the Airdrop.

Either of these platforms can be used in the stressed or unstressed condition. For the unstressed condition the parachute is attached to the load and the platform merely serves to hold the cushioning in place. For the stressed condition the parachute is attached to the platform and the load is stacked on the platform. This configuration is used for loads such as rations and fuel cans which do not have sufficient structure for attachment of the parachute. For this study attention will be focused on stressed platforms of both types.

The Type II platform shown in Fig. 4 is a composite type structure made, as previously mentioned, of aluminum and balsa wood sandwich type modules. These modules may be grouped in two's, three's, four's, or whatever is required for the load. The modules are connected together by two heavy aluminum rails along the edges of the short sides. These rails provide tie points for the suspension slings and for the load tie down straps. The sandwich part of the module consists of a 2 1/2 in. balsa wood core, or slab, bonded with epoxy to two aluminum skins 0.05 in. thick. (See Fig. 4). Around the perimeter of the balsa wood is an aluminum frame made up of two square tubular shaped members on the short sides and two channel shaped members on the long sides. This frame is both riveted and adhesive bonded to the aluminum skins. The balsa wood used in the core is end grain cut and is only used as a shear carrier. Its primary purpose is to hold the two sheets of aluminum at the desired distance apart and to prevent their buckling. This structure is light, yet quite rigid. As can be seen from the figures and the above description the platform is not exactly a true plate, nor is it a frame. It is a combination of both.

The Type IV platform shown in Fig. 5 is made up of two 1/2 in. plywood sheets and 2 in. x 6 in. x 9 ft planks connected between two heavy side rails. Each module consists of five planks and the plywood sheets which are nailed to the top and bottom of the planks. To assemble a platform the desired number of modules are placed side by side. These modules are then bolted to the side rails. The 2 in. x 6 in. planks or stringers extended beyond the plywood sheets for this purpose. In the assembly only three planks per module (the two exterior planks and the center plank) are bolted to the side rails. Three bolts fasten each end of each plank to the side rails.

The modular construction of the platform, regardless of whether it is the Type II or the Type IV platform makes

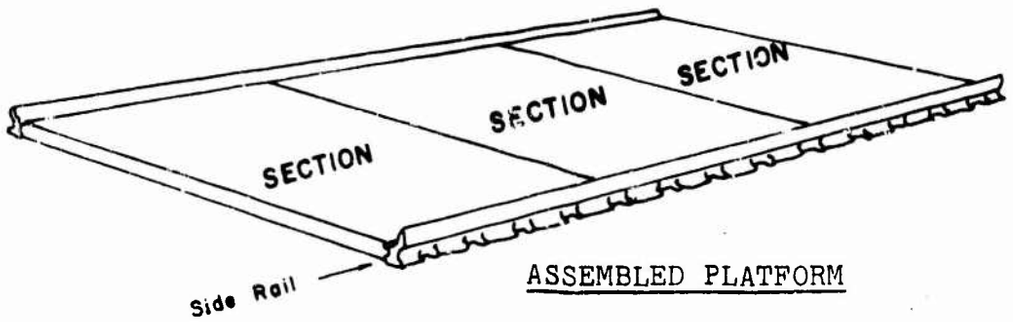

ASSEMBLED PLATFORM

Aluminum skin is glued (Epoxy) to balsa wood and is riveted to outer frame.

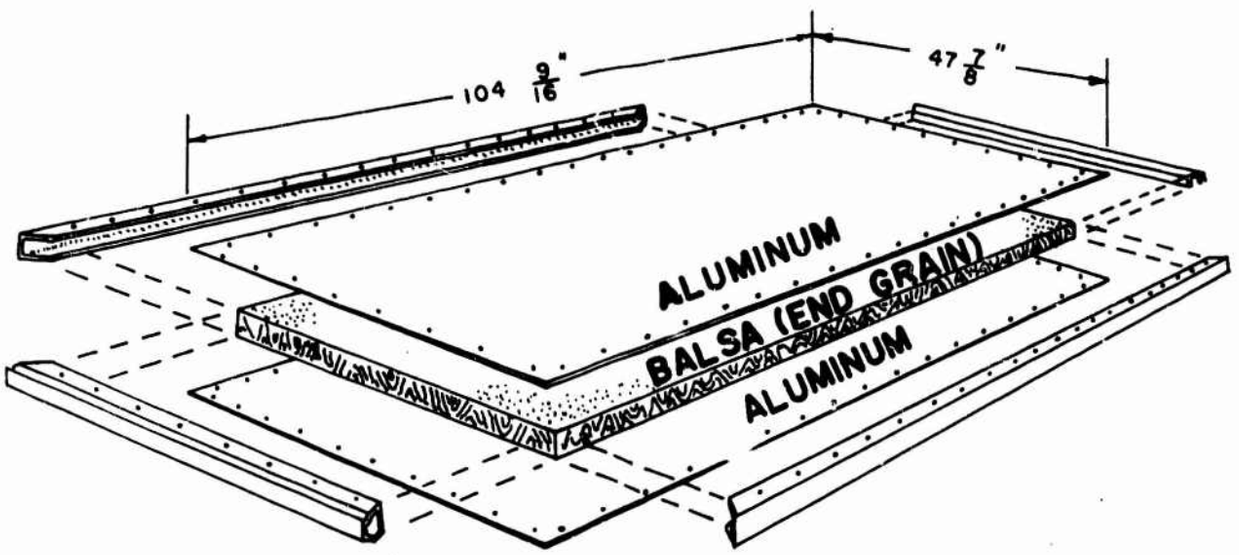

TYPE II MODULAR SECTION

ASSEMBLY

Fig. 4 Platform and Module Assembly.

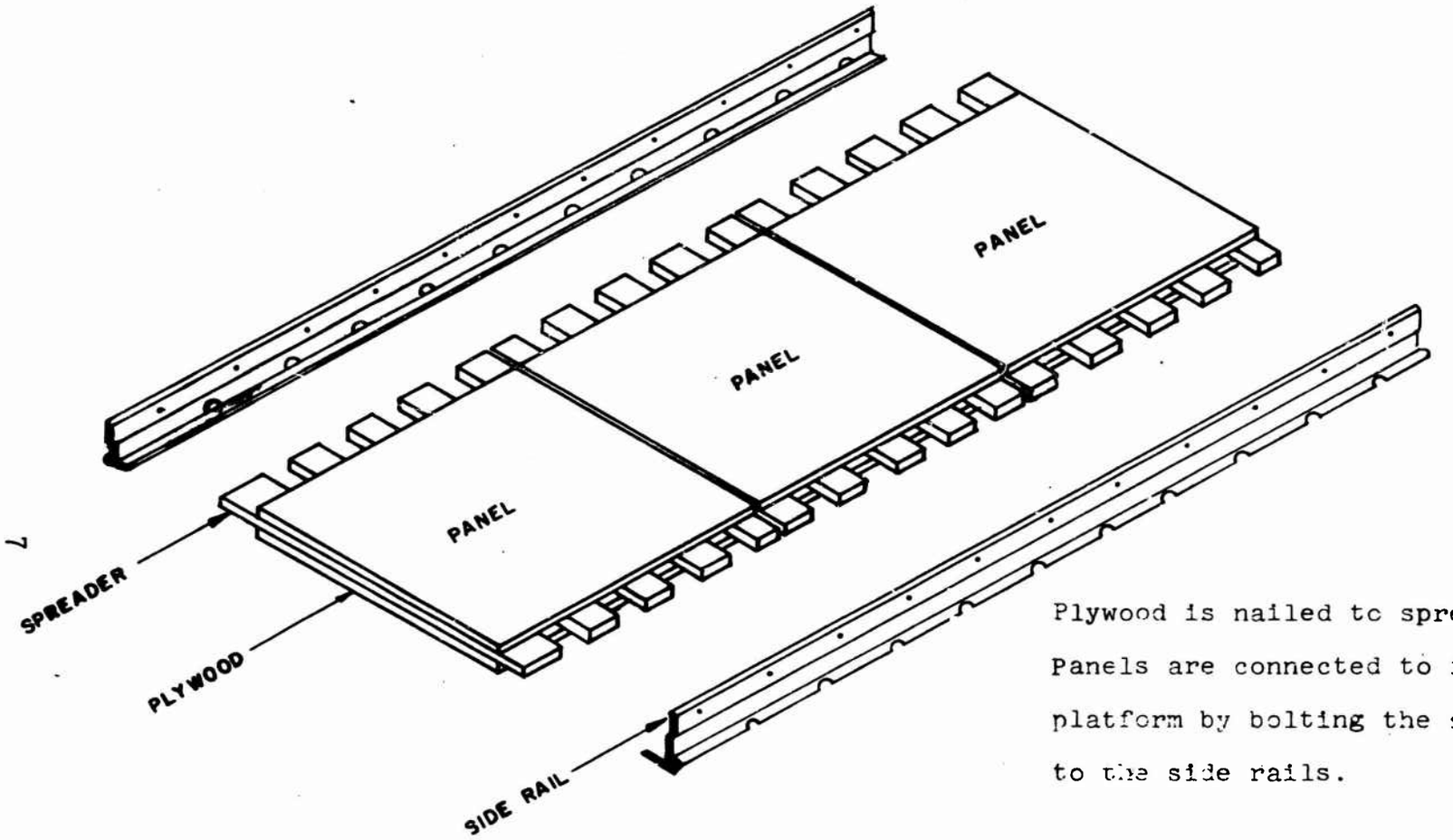

Plywood is nailed to spreaders. Panels are connected to form platform by bolting the spreaders to the side rails.

Fig. 5 Type IV Platform and Module Assembly

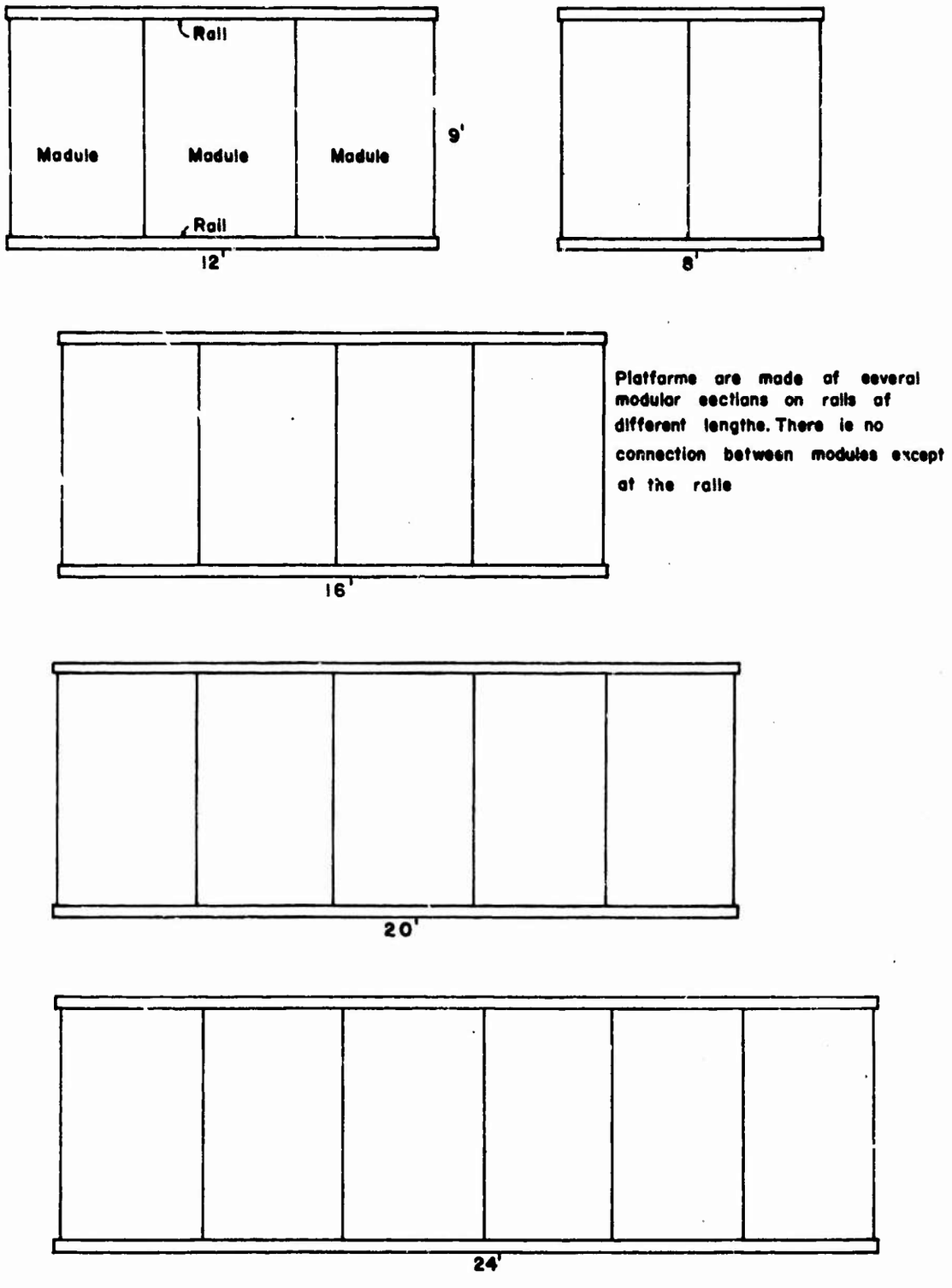

Fig. 6 Typical Platform Dimensions

it a simple matter to fabricate several different sizes of platforms. All modules are 4 ft x 9 ft in size, and the rails are of lengths divisible by 4, ranging from 8 ft to 24 ft, as shown in Fig. 6. A platform can be readily made up to any desired size by simply assembling the required number of modules to the two side rails so long as the structural conditions such as stress and deflection are properly taken into consideration.

3. Analysis

a. Static Loading

A platform made up of modules as described above can be considered to be a plate but obviously a very nonhomogeneous plate with very unusual boundary conditions. For analysis the plate is considered to be a planar network of beams similar to the one shown in Fig. 7. The beams are

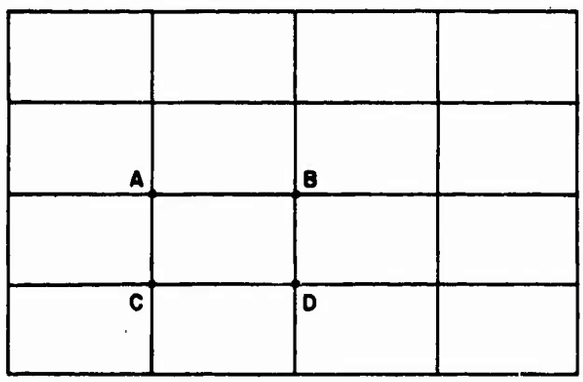

Fig. 7 Example of Grid Layout.

assumed to be rigidly connected at the joints and all loads are normal to the plane of the network, and loads are applied only at the joints. This same concept can be used for both static and dynamic loading if the inertia loading is added to the static loading at each joint.

The stresses and deflections produced by static loading are not of direct interest in this problem since these quantities can easily be measured if they are required.

However, the approach to the problem of obtaining the dynamic stresses and deflections has been to estimate the beam stiffness properties which are needed by the computer for generating the stiffness matrix, compute the static deflections using this information, and then compare the computed deflections to corresponding measured static deflections. In general these deflections should not be expected to agree perfectly since the beam stiffness properties are only estimates and the representation of the platform by the beam network is an approximation. Therefore, after the comparison is made the stiffness properties are altered in the way estimated to be necessary to bring the two sets of deflections into agreement. The deflections are then recomputed and compared again with measured values. This process is repeated until satisfactory agreement is obtained. The final stiffness properties are then assumed to be an adequate representation of the platform characteristics for use in the analysis of stresses produced by dynamic loading.

b. Formulation of the Problem

Consider the basic grid element (beam shown in Fig. 8). The coordinates ξ_1, ξ_2 and ξ_3 shown on this element, referred to as member coordinates always have directions as shown, with respect to the member, i.e. ξ_1 is along the axis of the member, ξ_2 is in the plane of the platform and ξ_3 is normal to the plane of the platform. Positive directions for this coordinate system are indicated by the arrows. For each beam element there are six possible

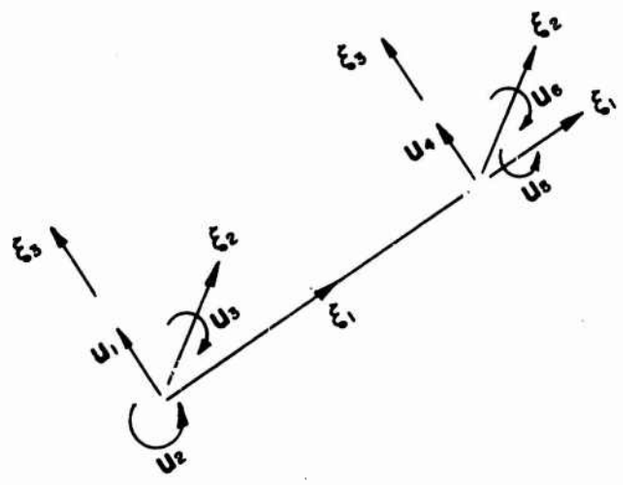

Fig. 8 Grid Element Displacements.

displacements, u_1 and u_4 are vertical displacements, u_2 and u_5 are rotations corresponding to torsion, and u_3 and u_6 are rotations produced by bending moments. These displacements are related to the corresponding displacements of the other beams in the network by the continuity requirements at each joint. Thus it is seen a load applied at any joint in the network will produce changes in the displacements at every joint unless there are constraints. The relationship between displacements, beam properties and loads for a single isolated beam can be written as

$$a_{11} u_1 + a_{12} u_2 + a_{13} u_3 + a_{14} u_4 + a_{15} u_5 + a_{16} u_6 = p_1 \quad (1)$$

Since there are six such equations for each beam they are more conveniently written in matrix form

$$\begin{bmatrix} a_{11} & a_{12} & \cdots & a_{16} \\ a_{21} & a_{22} & \cdots & a_{26} \\ \vdots & \vdots & & \vdots \\ a_{61} & a_{62} & \cdots & a_{66} \end{bmatrix} \begin{bmatrix} u_1 \\ \vdots \\ u_6 \end{bmatrix} = \begin{bmatrix} p_1 \\ \vdots \\ p_6 \end{bmatrix} \quad (2)$$

where a_{ij} means the force or moment which must be applied in the direction of u_i to maintain zero displacement there when a unit increment is given to u_j and all other degrees of freedom are restrained. For example, a_{11} is the force which must be applied in the direction of u_1 to produce a unit deflection of u_1, with all other degrees of freedom restrained. Likewise a_{62} is the bending moment which must be applied in the sense of u_6 to maintain u_6 unchanged when u_2 is given a unit increment with the other 5 degrees of freedom restrained. These coefficients can be computed if the bending stiffness and the torsional stiffness of the beam are known. p_i is the external force or moment corresponding to u_i of the isolated beam.

When all the member stiffness matrices (the array of a_{ij} values) have been obtained the stiffness matrix of the entire network can be computed. The basic principle involved is the compatibility of deflections at the joints. Deflections and loads for the network are related by a matrix equation of the same form as the one given for the single beam. Thus

$$\begin{bmatrix} K_{11} & K_{12} & \cdots & K_{1n} \\ K_{21} & K_{22} & \cdots & K_{2n} \\ \vdots & \vdots & & \vdots \\ K_{n1} & K_{n2} & \cdots & K_{nn} \end{bmatrix} \begin{bmatrix} U_1 \\ U_2 \\ \vdots \\ U_n \end{bmatrix} = \begin{bmatrix} P_1 \\ P_2 \\ \vdots \\ P_n \end{bmatrix} \quad (3)$$

where [K] is the stiffness matrix for the network of beams and K_{ij} is the force or moment at the i^{th} degree of freedom due to unit displacement U_j when all degrees of freedom are restrained except the j^{th}. [U] is the displacement matrix which is the unknown quantity in the matrix equation. [P] is the force or moment matrix which represents the external forces and moments applied to the structure. After [U] is found the forces and moments can be computed using the equilibrium equations for each member as given above.

$$[a]\,[u] = [p] \qquad (2)$$

From this brief discussion of the computation procedure it is seen that the starting point is the determination of the stiffness properties of each beam in the grid. However, the ordinary methods used for calculating the moment of inertia (I) and the torsional constant (K) cannot be applied directly because the effective cross section is indeterminate, and the material is in general nonhomogeneous. Approximate values for I and K are computed however, using the ordinary method. A computer program published in 1962 by the Jet Propulsion Laboratory [2] is used for performing all other computations for static deflections. Input information required, includes I, the moment of inertia for each beam, K, the torsional constant for each beam, the joint coordinates, the modulus of elasticity, Poisson's ratio, and the loads. The output includes the stiffness matrix, load matrix, static deflections, and static stresses. Once the input data have been properly prepared for entering the computer the deflections and stresses are quickly and easily computed. As indicated above the computed deflections are compared with measured deflections to determine how the input properties should be modified to make the beam network properly represent the platform.

c. Experimental Technique and Results

The actual loading of the platform during an airdrop, as seen in Fig. 2 subjects the platform to three force components at each sling attachment, two in-plane components, and one normal component. Only the vertical component is considered in the computation since the in-plane components contribute insignificantly to the moments and stresses. This can be seen by comparing the moments produced at the midpoint of the platform by the vertical and in-plane components, assuming a deflection of 1 in. at the midpoint, with respect to the points of support. For the experimental measurements on the Type II platform the platform was supported on four spherical balls near the points where the suspension slings

would ordinarily be connected, and a concentrated load of 1000 lb was applied at the center of the platform in the direction normal to the surface of the platform. A hydraulic jack reacting against a strut hanging from a jib crane presses down against the platform causing it to deflect downward. The jib crane will swing over any desired point on the platform. The strut is hung on the boom of the crane on a roller so that it can be moved back and forth along the boom easily. This gives the loading system a two dimensional positioning capability. A counter weight hung on the outer end of the crane helps counteract the 1000 lb. upward force from the jack since the tension strap on the jib cannot resist large compressive forces. See Fig. 9.

For the Type IV platform, the same procedure was followed except the applied concentrated load was reduced to 500 lb.

The two essential measurements made were (1) the deflections, and (2) the applied load. To measure the deflection a dial gage mounted on a frame is used. This frame rests on the floor under the platform, and can be moved to any point for deflection measurements. To make a measurement it is necessary to first position the dial gage at a selected grid point. With no load on the platform the gage is read. Then the load is applied and the gage is again read. Thus the platform is loaded and unloaded for each deflection measurement.

The load is measured by a load cell mounted between the hydraulic jack and the platform. For these measurements a 2000 lb capacity load cell was used in conjunction with a differential d.c. amplifier and a digital voltmeter as shown in Fig. 10.

d. Stiffness Properties of the Platforms

Symmetry of the platform and loading makes it necessary to consider only one quarter of the platform in the calculation and measurement of the deflections. Grid layouts for the two types of platforms are shown in Figs. 11 and 12. The spacing of both grids are irregular because it is necessary to take joints and beams close together in those regions where platform properties change rapidly, i.e., near the side rails, and along adjoining edges of modules. Typical cross sections of grid elements were selected for computations of I and K. These cross sections are shown in Fig. A1 through A14 in Appendix A. For the Type II platform, the balsa wood core is assumed to contribute nothing to the rigidity. Only the aluminum parts of the cross section are considered.

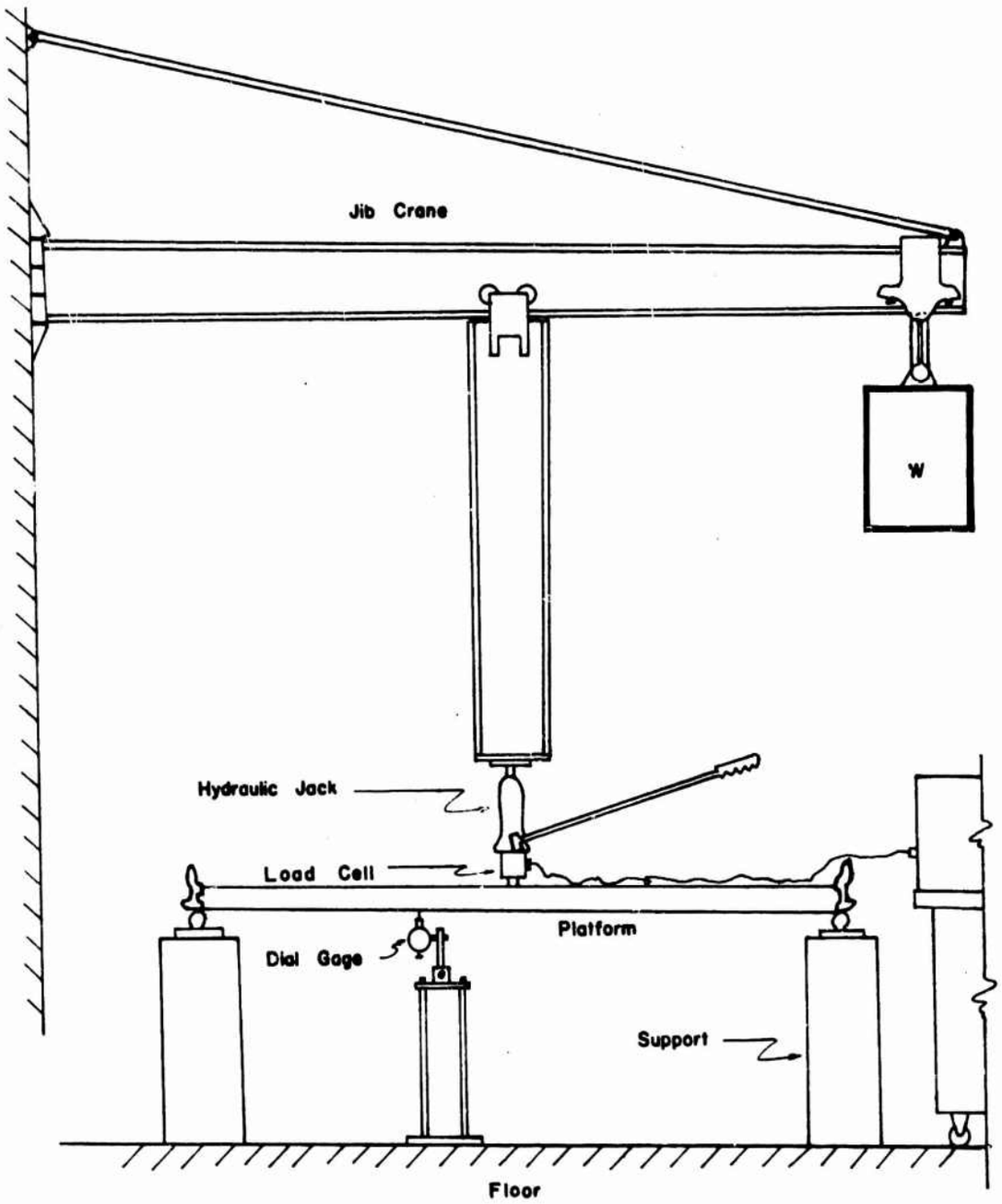

Fig. 9 Laboratory Loading Set-Up.

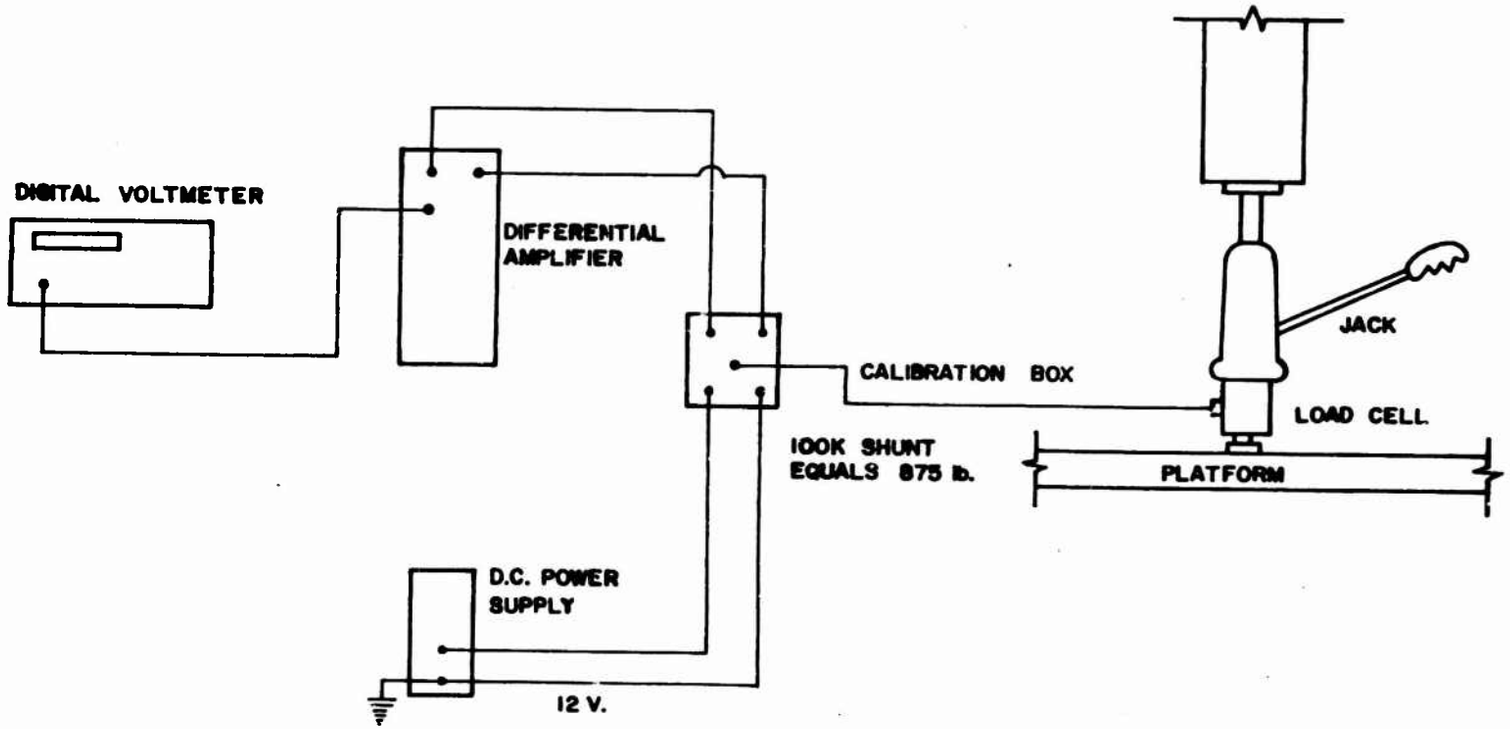

Fig. 10 Electrical Instrument Circuit.

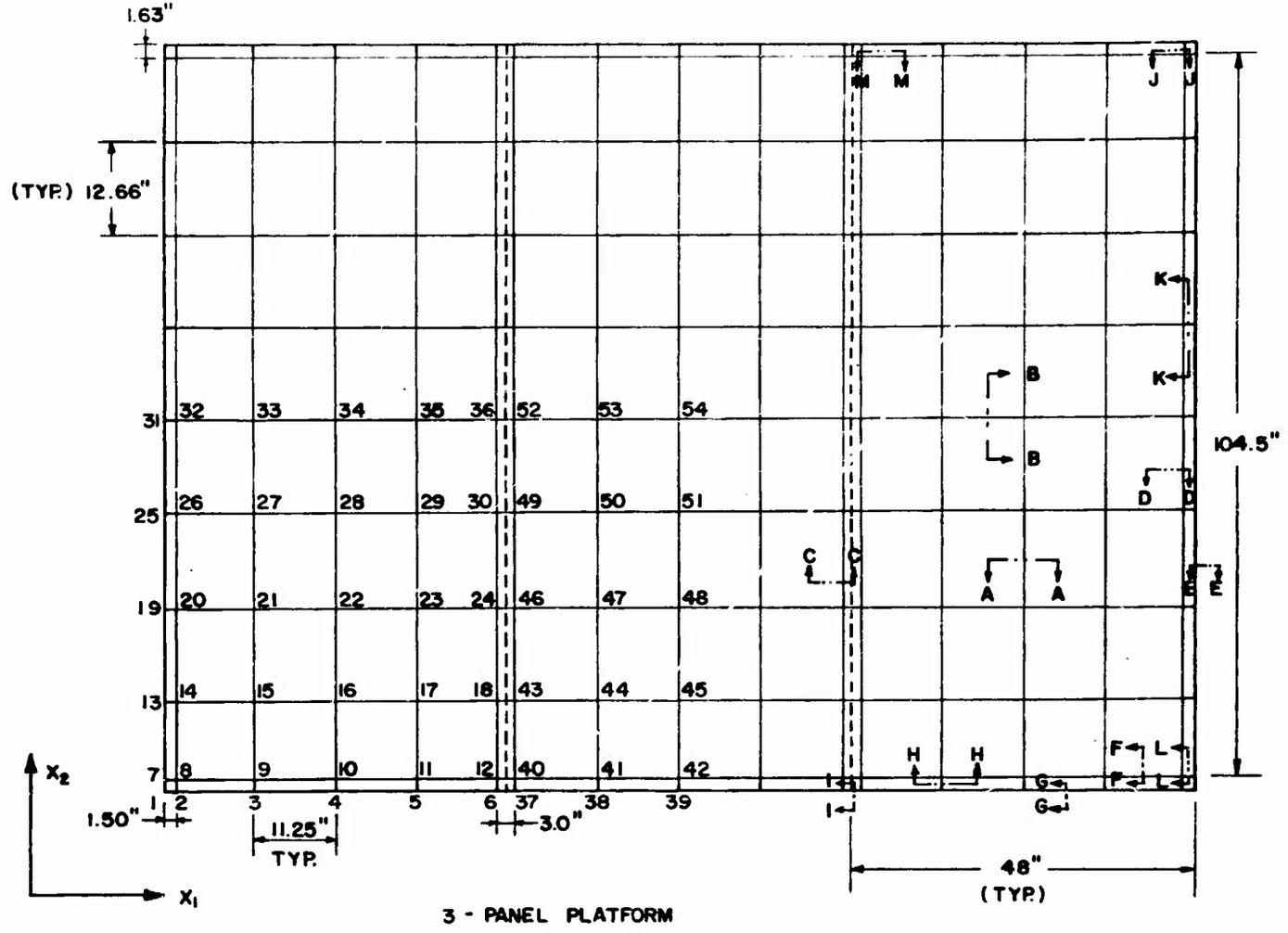

Fig. 11 One-Quarter Grid Layout of Type II Platform.
For Cross Sections See Appendix B.

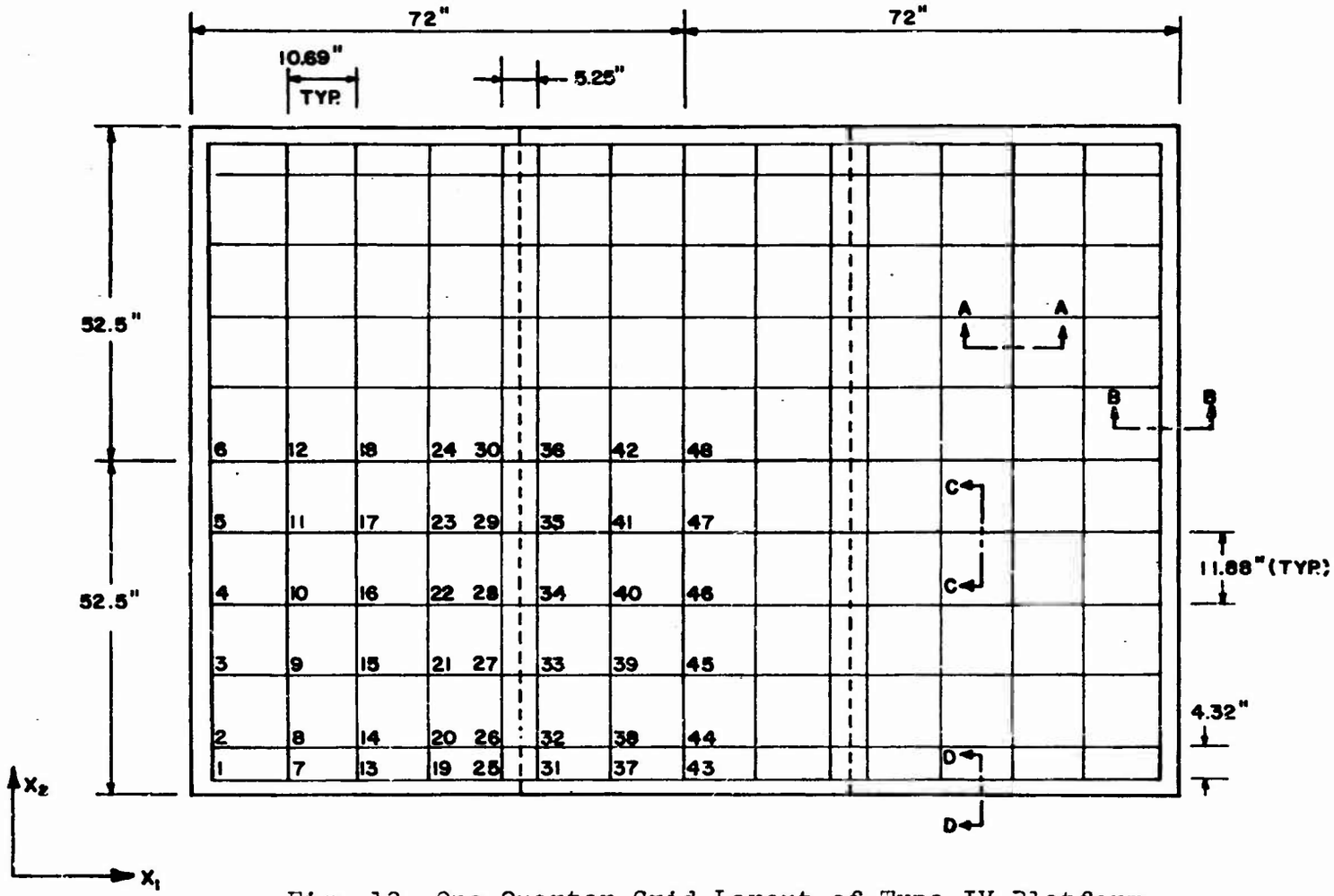

Fig. 12 One-Quarter Grid Layout of Type IV Platform. For Section Cuts see Appendix B.

To estimate I and K, the cross sections are divided into a group of rectangles. Then for I the parallel axis theorem as expressed in the following equation is applied to these rectangles.

$$I_{x_i} = \Sigma\left(\frac{bh^3}{12} + Ad^2\right)$$

where b is the base of the rectangle and h is the height. A is the cross sectional area and d is the distance from the reference axis of each element to the reference axis of the whole cross section. To estimate K, the equation for a narrow rectangle[3] is applied.

$$K = \Sigma\frac{bt^3}{3}$$

where b is the width or length, and t is the thickness of the rectangular elements.

Material properties used for the computation of deflections are:

Type II platform

1. Modulus of elasticity for aluminum

$$E = 10 \times 10^6 \text{psi}$$

2. Poisson's ratio for aluminum

$$\nu = 0.3$$

Type IV platform

1. Modulus of elasticity for Douglas fir[4,5]

$$\text{Equivalent } E = 1.6 \times 10^6 \text{ psi}$$

2. Poisson's ratio

$\nu_{lt} = 0.37$ perpendicular to grain

$\nu_{tl} = 0.03$ parallel to the grain

After I and K have been estimated for all grid elements, these data, and a concentrated force of 1000 lb at the center of the platform together with other required information, are read into the computer. As indicated previously the computed deflections are tc be compared with the measured values.

By a trial and error procedure, the I and K of the grid elements are adjusted until the differences between computed and measured deflections are acceptable. Then a set of stiffness properties representing Type II platform stiffness is determined. This set is shown in Table IIIB of Appendix B.

The same procedures used for the Type II platform were applied to the Type IV platform. Typical cross sections of the grid elements are shown in Fig. 13A and 14A of Appendix A. A set of stiffness properties representing the Type IV platform are shown in Table IVB of Appendix B. A comparison of the deflections of both types of platforms based on the final adjusted set of stiffness properties, and measured values is made in Tables IB and IIB of Appendix B.

It may be noted in Table IB that two points on the platform actually deflect upward as the load is applied. Both the computations and the experiments show this. Also it may be noted that at some points the calculated deflection exceeds the measured deflection and at other points the situation is reversed. This indicates that further adjustment of stiffnesses will not improve the agreement. This observation can be made because in general changing the stiffness of a single beam element has very little effect on deflections. To produce a significant change in the deflection at a given point a general change in stiffness is required. Once the state is reached where some deflections are greater and some less than the measured values, further changes in stiffness tend to improve the agreement at some points and to worsen it at others.

e. Further Static Loading Calculations

1) Type II Platform. A uniform load of 106.1 lb per sq ft was distributed over an area bounded by lines 6 in. from each edge of the platform. This gives a total resultant load of 9000 lb. Since the computational procedure requires that loads be applied at the grid points the distributed load is approximated by applying at each grid point a load equal to one-fourth of the total load acting on the four rectangular sections of the grid adjacent to the point. Calculations of stresses and deflections were made with the point of support at grid points 2, 3 and 4. For the computations the points of support must coincide with a grid point.

If the support is under grid point 2, which is on the side rail 1.5 in. from the end of the platform the maximum

computed stress is 40,500 psi and the deflection at the center of the platform is 3.334 in. The maximum stress occurs in the side rail. If the support is placed under point 3, which is 12.75 in. from the end of the platform, the maximum stress is reduced to about 2/3 of the value computed for the previous case, and the deflection at the center is reduced to 1.89 in. For the support at point 4, 24 in. from the end of the platform, the maximum stress is about 1/2 the value obtained for the support at point 3, and the deflection at the center is 0.994 in.

Bending moments and deflections along the grid lines for supports at points 2, 3 and 4 are shown in Figs. 1C through 9C, Appendix C.

2) Sign Convention The sign convention for moments, forces and deflections, in the computer printout are explained as follows. Global Coordinates X_1, X_2 and X_3 (X_3 perpendicular to the plane of the grid) are as shown in Fig. 13.

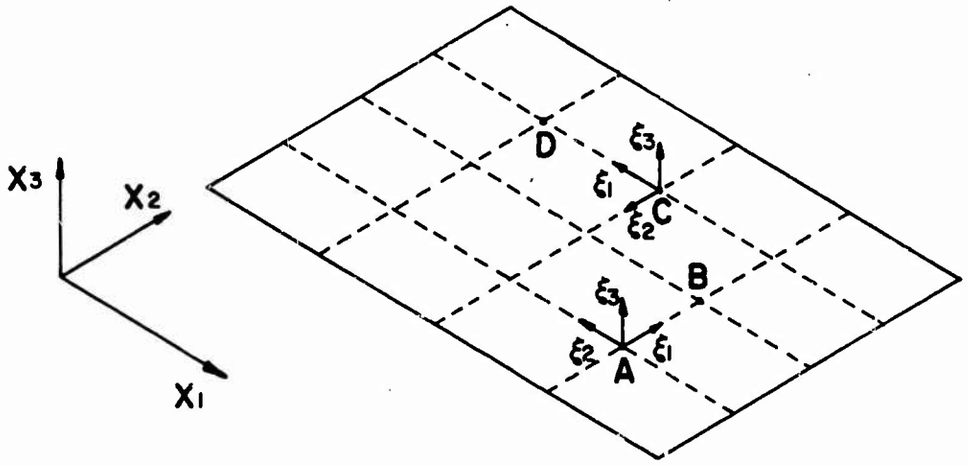

Fig. 13 Global Coordinates and Member Coordinates for Members AB and CD.

These are fixed coordinates which follow the right hand rule. The member coordinate system (ξ_1, ξ_2, ξ_3) shown in Fig. 13 also follows the right hand rule. It is the sign convention associated with member coordinates that determines the signs of moments and forces in the computer printout. In this system, ξ_1 is always along the member, ξ_3 is always perpendicular to the plane of the grid and positive upward, ξ_2 is

determined by the right hand rule. As an illustration consider member AB (from A to B) shown in Fig. 14. BM-A

Fig. 14 Signs of the Moments and the Forces of Member AB

indicates bending moment at A, TM indicates torque and V is shear force. Positive directions for these quantities at both A and B are shown in Fig. 14. For the member CD (from C to D) the axes and positive directions are shown in Fig. 15.

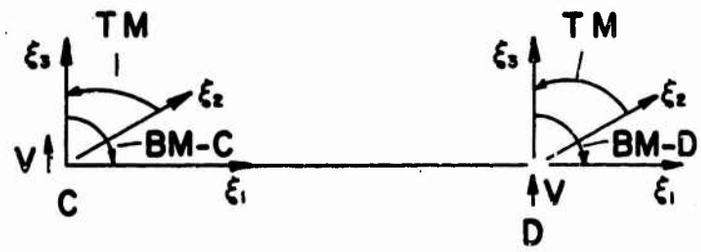

Fig. 15 Signs of the Moments and the Forces of Member CD

Bending stresses in any member can be computed from the bending moments shown in Fig. 1C - 9C by using the

appropriate moment of inertia selected from Table IIIB of Appendix B, and the cross sectional dimensions in Fig. 1A through 12A, in the usual bending stress expression.

$$\sigma = \frac{Mc}{I}$$

3) Type IV Platform This platform was loaded with a total resultant load of 7000 lb uniformly distributed over the same area used for the Type II platform, namely that area bounded by a line 6 in. from each edge of the platform. This loading was approximated, as it was for the type II platform by applying one-fourth of the loading acting on the four rectangles adjacent to each grid point as a concentrated load on the point.

Supports were placed under point 1 and then point 7. Point 1 is on the side rail 2.6 in. from the end of the platform and point 7 is on the rail 10.7 in. from the end. With the support at point 7 the maximum bending moment in each spreader occurs at the center (points 12, 18, 24, 30, 36, 42, 48). Furthermore these bending moments are essentially the same in each spreader with the exception of point 12. There the moment is about 30% less than the moments in the other spreaders. This is undoubtedly due to this point being near the unloaded edge of the platform. The maximum bending moments in the X_2 direction (transverse) and the X_1 direction (longitudinaly) are about 1080 in.-lb and 34 in.-lb, respectively. In the side rail the maximum bending moment occurs at point 43, the center of the span. It is 6290 in.-lb. and the maximum stress is 2880 psi. Deflection at the center of the platform is 0.315-inch. If the platform behaves elastically, as is assumed in these calculations, all moments, stresses, and deflections would be increased by a factor of N if the loading is increased by that factor. As a matter of fact the platform does not behave in a linear fashion and if the load were to be multiplied by a factor of 4 the deflections would probably be somewhat less than 1.3 in. (4 x 0.315), since the platform appears to become stiffer as deflections increase. On the other hand the moments would probably be close to 4 times as large as those given since moments depend on equilibrium requirements and are not appreciably affected by displacements.

For the support at point 1 (2.6 in. from the end of the platform) the bending stress in X_2 direction differed by less than 2% from the stresses calculated with the support at point 7, and in the X_1 direction the maximum stress was

increased to 340 psi. In the side rail the maximum bending moment increased to 8900 in.-lb. and the bending stress to 4080 psi. Deflection at the center of the platform is 0.478 inch.

These computations indicate a marked difference in the behavior of the two platforms, and sensitivity to the location of the point of support. It should be noted that the Type IV platform is much more anisotropic than the Type II platform and the material properties for the former are much more poorly defined than they are for the latter.

2. Dynamic Analysis

a. Principle

In the dynamic analysis a lumped mass representation is used for the platform and its loading. There are three degrees of freedom (vertical deflection and two rotations) at each grid point. An equation of motion must be written for each degree of freedom. As an example consider the free body diagram for the i^{th} degree of freedom in vertical deflection as shown in Fig. 16.

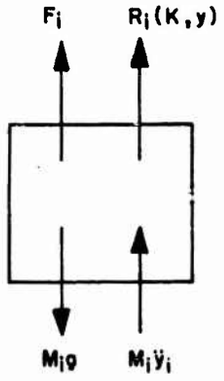

Fig. 16 Free Body Diagram for a Vertical Degree of Freedom.

For this free body the equation is

$$\ddot{y}_i = \frac{M_i g - F_i - R_i(K,y)}{M_i} \qquad (4)$$

where $\ddot{y}_i$ = the acceleration of the mass M_i
g = acceleration of gravity
F_i = force applied in the vertical direction
$R_i(K,y) = \sum_{j=1}^{N} K_{ij}y_j$, K_{ij} are the i^{th} row

elements in the stiffness matrix of the platform, y_j is displacement for each degree of freedom, and N is the total number of degrees of freedom.

The equation of motion for a rotational degree of freedom has the same form as that for the vertical degree of freedom. But in that case M_i is mass moment of inertia, $\ddot{y}_i$ is angular acceleration, g is zero, F_i is applied moment and $R_i(K,y)$ is the resisting moment due to platform stiffness.

At time t, if the displacement and velocity for all degrees of freedom are known, the acceleration can be calculated by the above equations. At time $t + \Delta t$, the velocity and the displacement can be obtained by numerical integration using the velocity and acceleration at time t. The technique used for the integration, the Runge-Kutta-Gill method[6] is outlined as follows:

let
$$\dot{y}_n = v$$
and
$$\ddot{y}_n = f(t,y)$$
then
$$\dot{y}_{n+1} = \dot{y}_n + \frac{\Delta t}{6}(m_o + 4m_1 + m_2)$$
and
$$y_{n+1} = y_n + \Delta t\, \dot{y}_n + (\frac{\Delta t}{6})^2 (m_o + 2m_1)$$
where
$$m_o = f(t_n, y_n)$$
$$m_1 = f(t_n + \frac{\Delta t}{2}, y_n + \frac{\Delta t}{2}\dot{y}_n)$$
$$m_2 = f(t_n + \Delta t, y_n + \Delta t\, \dot{y}_n)$$

in this way, the acceleration, the velocity, and the displacement of each degree of freedom at any time can be obtained if the initial conditions, velocity and displacement at t = 0, are known. The time increment, Δt is determined by trying increasingly smaller values until the convergence of the computed results is acceptable.

b. Type II Platform

1) Loading. The same loading used for static analysis was applied, i.e. the total load of 9000 lbs is

uniformly distributed over a central rectangular area with the boundaries 6 in. from the edges of the platform. The applied dynamic force, which is a function of time is due to the shock of the parachute opening. The force in the right aft sling shown in Fig. 3 was selected for application at grid point 3 which is on the side rail 12.75 in. from the end. As indicated in Fig. 3, actual sling forces during an airdrop are not evenly distributed among the four slings with respect to either time or magnitude. This is a consequence of platform rotational displacement relative to the alignment of the parachute at the instant when inflation begins. In the following analysis, the sling forces are assumed to be equal in order to take advantage of symmetry. This is believed to be a valid first approximation and in fact may be a conservative assumption if the most critically loaded sling is used as the basis for the force time history at each suspension point.

2) Stiffness and Mass Matrices. The stiffness properties of the platform obtained in the static loading tests were used. Symmetry of both load and platform make it necessary to consider only 1/4 of the platform. There are 54 grid points in the quarter platform which is the same as in the static analysis. Since each grid point has three degrees of freedom, the size of the stiffness matrix is 162 x 162.

For the rotational degree of freedom at each grid point and the vertical degree of freedom at the unloaded grid points around the edges of the platform, the corresponding mass moment of inertia, and mass are very small. This causes computational difficulties due to the form of equation (4). To avoid this trouble the rotational degree of freedom and some of the vertical degrees of freedom around the edges of the platform are eliminated. This is done by working with the strain energy and obtaining a condensed stiffness matrix. The basic steps in the procedure are outlined as follows beginning with the strain energy U in an N degree of freedom system[7].

$$U = 1/2 \, [y_1 \; y_2 \; - \; - \; - \; y_n] \, [K] \begin{bmatrix} y_1 \\ y_2 \\ \vdots \\ y_n \end{bmatrix}$$

where y_i is the displacement of the i^{th} degree of freedom, either vertical displacement or rotation, [K] is the stiffness matrix.

The condition that minimizes U with respect to y_s is

$$K_{s1}y_1 + K_{s2}y_2 + - - - + K_{ss}y_s + - - - + K_{sn}y_n = 0 \quad (6)$$

Solve for y_s and substitute into the equation for U. This gives a modified stiffness matrix [K*] with row and column S deleted.

$$K^*_{ij} = K_{ij} - K_{is}\ (K_{js}/K_{ss}) \quad (7)$$

For the mass matrix the corresponding masses of the remaining degrees of freedom are retained and those of the eliminated degree of freedom are omitted.

3) Comparison of Displacements Calculated with 29 and 36 Degrees of Freedom. For the purpose of checking the accuracy of the results obtained using different numbers of degrees of freedom, 29 and 36 degrees of freedom were tried. All the degrees of freedom are vertical displacements. Thus the degree of freedom may be identified by the grid point associated with it. The 36 degree of freedom system contains grid points 3, 9, 10, 11, 12, 15, 16, 17, 18, 21, 22, 23, 24, 27, 28, 29, 30, 33, 34, 35, 36, 40, 41, 42, 43, 44, 45. 46, 47, 48, 49, 50, 51, 52, 53, 54, and the 29 degree of freedom contains grid points 3, 15, 16, 17, 18, 21, 22, 23, 24, 27, 28, 29, 30, 33, 34, 35, 36, 43, 44, 45, 46, 47, 48, 49, 50, 51, 52, 53, 54. In general, the displacements calculated using 36 degrees of freedom are larger than those calculated with 29 degrees of freedom. Fig. 17 shows the displacements of point 3 (the support) and point 54 (the center of the platform) calculated using 29 and 36 degrees of freedom. These displacements include the rigid body displacement with all displacements being zero at the time when the action of the main parachute starts. The relative displacement of point 54 with respect to point 3 is shown in Fig. 18a.

The negative relative displacement that first appears at about 0.3 secs after the retarding force application begins indicates that the center of the platform is above point 3 where the sling is attached. Referring to Fig. 3 it is seen that the sling force drops to zero at about 0.3 secs and remains at zero until about 0.5 sec, the approximate time at which point 54 again drops below point 3. That the negative relative displacement should coincide so closely with the time of zero force is not just a happenstance. It

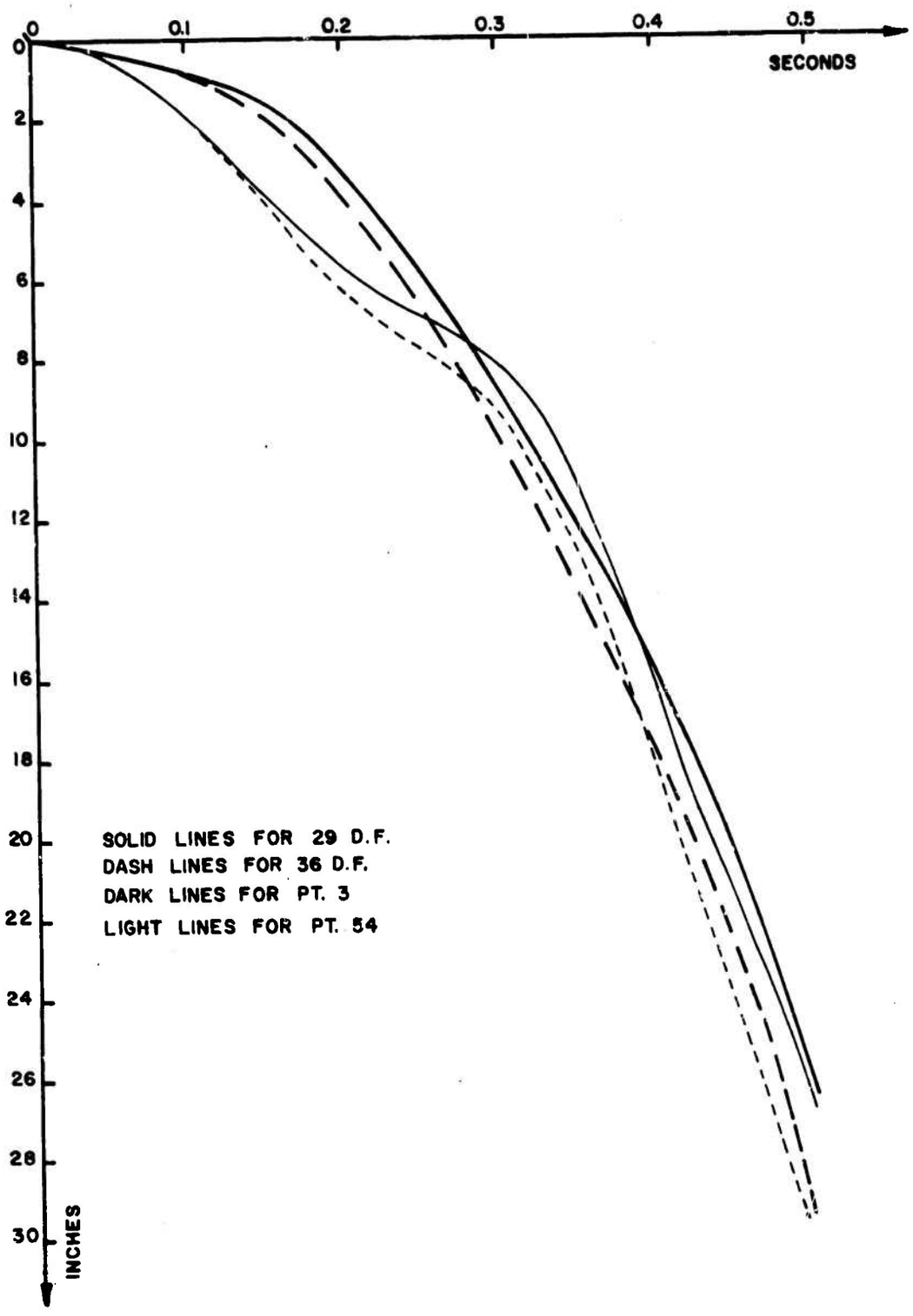

Fig. 17 Displacements of Points 3 and 54 Calculated for 29 and 36 Degrees of Freedom.

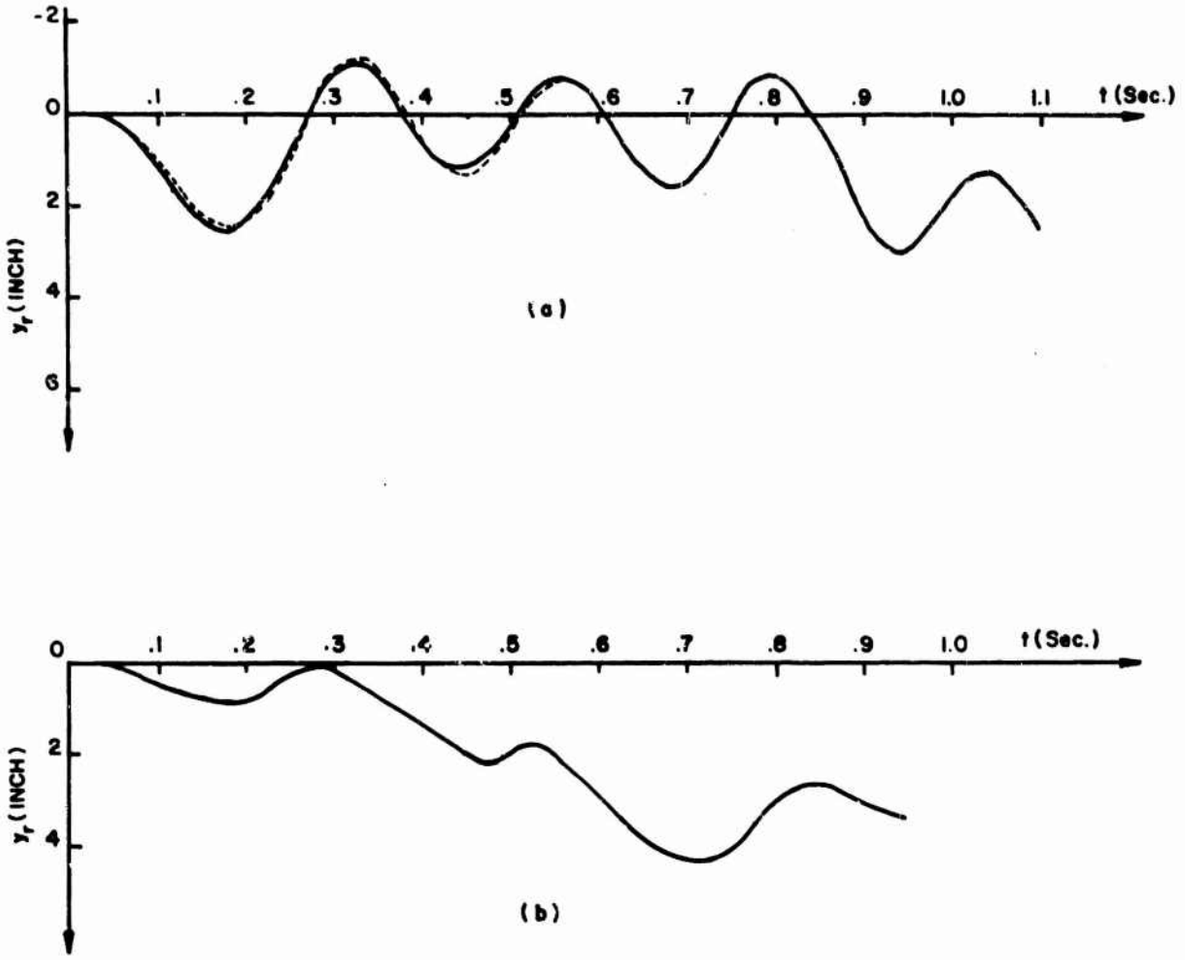

Fig. 18 (a) Displacement of Point 54 Relative to Point 3 with Sus. Sling RT. AFT Force of Fig. 3, Applied at Point 3. Solid Line Indicates the Result for 29 Degrees of Freedom and Dash Line Is for 36 Degrees of Freedom.

(b) Applied Force Same as in (a) Except 0.45 Sec Taken as Starting Point for 29 Degrees of Freedom.

can be readily shown that a simple single degree of freedom system such as a tip loaded cantilever falling freely and then subjected to a rectangular acceleration pulse at the root will deflect with the mass always below the root while the acceleration pulse is being applied. However, after the acceleration pulse ends the mass can rise above the root, even though both continue to move downward, if the pulse duration is properly related to the natural period of the cantilever.

In view of this action of the simple system it does not seem unreasonable that a similar action might occur in the complex system represented by the platform. As further evidence of the validity of these results the relative displacements between points 54 and 3 shown in Fig. 18b were plotted using the force in the same suspension sling as the force input but starting application at 0.45 sec. The force does not vanish after that time, and as the plot shows point 54 never rises above point 3.

Using 29 degrees of freedom, it is found that the maximum deflection at the center of the platform, relative to point 3, is 5.17 in. This maximum occurs 1.2 sec after loading begins. The corresponding stress in the direction perpendicular to the side rail is about 24,500 psi, and parallel to side rail, 1,010 psi. The deflection shape of the platform is shown in Fig. 19. The relative deflection at each grid point indicated in the figure can be used to calculate the bending moment and then the bending stress along the grid lines.

Deflections at points on the rail can be obtained by extrapolation from the results shown in Fig. 19. However, the deflections at points 6 and 37 reflect the discontinuity in deflections which exists all along the line between the adjoining modules. This discontinuity cannot exist in the rail. If the extrapolated values are used to compute bending moments an abnormally high moment is obtained at points 6 and 37. This moment cannot be accepted as reliable.

3. Summary

The Type II and Type IV air drop platforms were approximated by a network of beams to compute the deflections, moments, and stresses developed in the platforms during the dynamic loading that results from deployment of the main parachute. Stiffness properties of the beams, I and K, needed for computing deflections and moments were calculated by the ordinary methods for determining these quantities

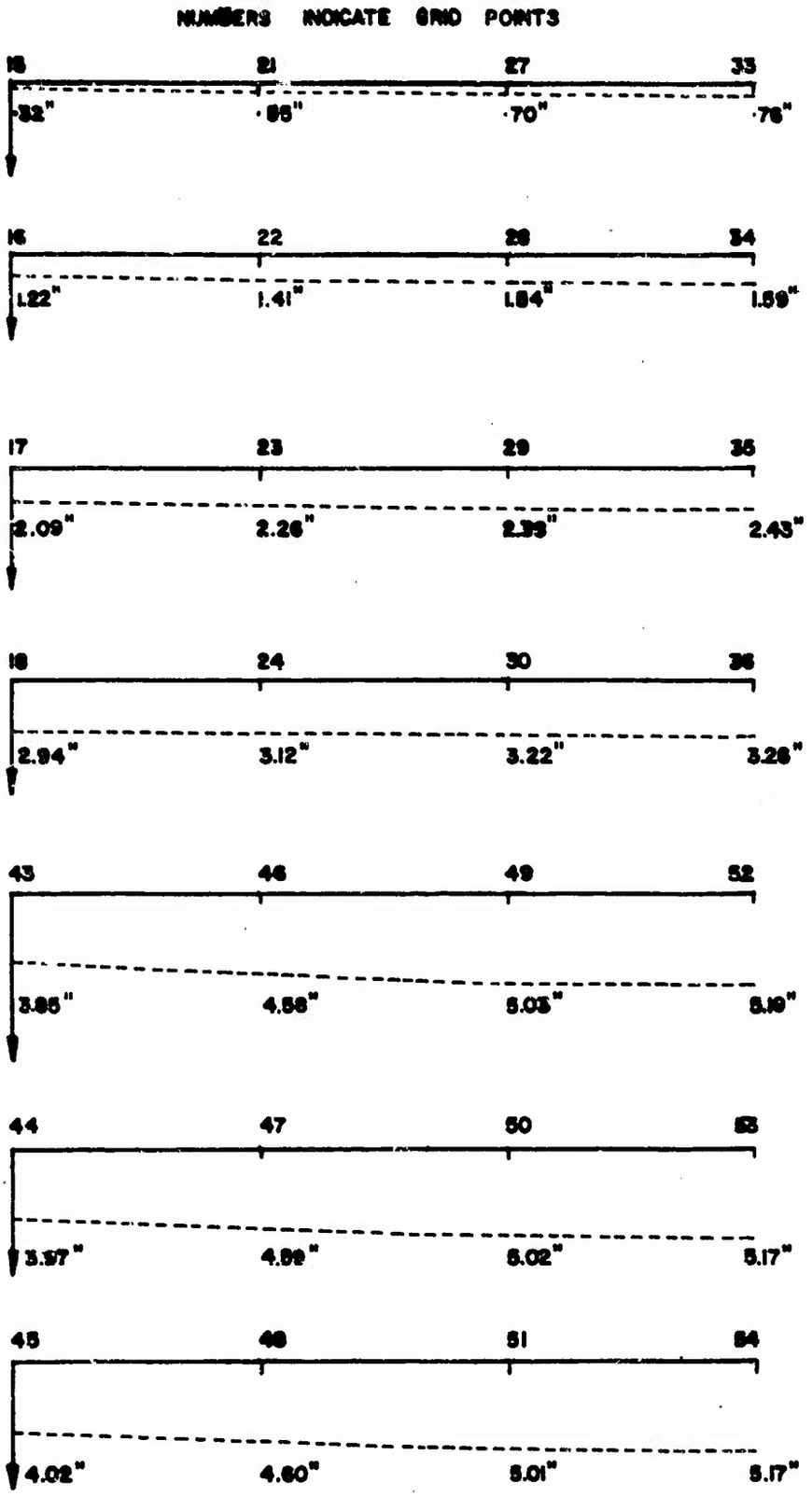

Fig. 19 Deflection, Relative to Point 3, of Type II Platform Due to Dynamic Loads when Point 54 Has Maximum Deflection (t = 1.2 Sec.).

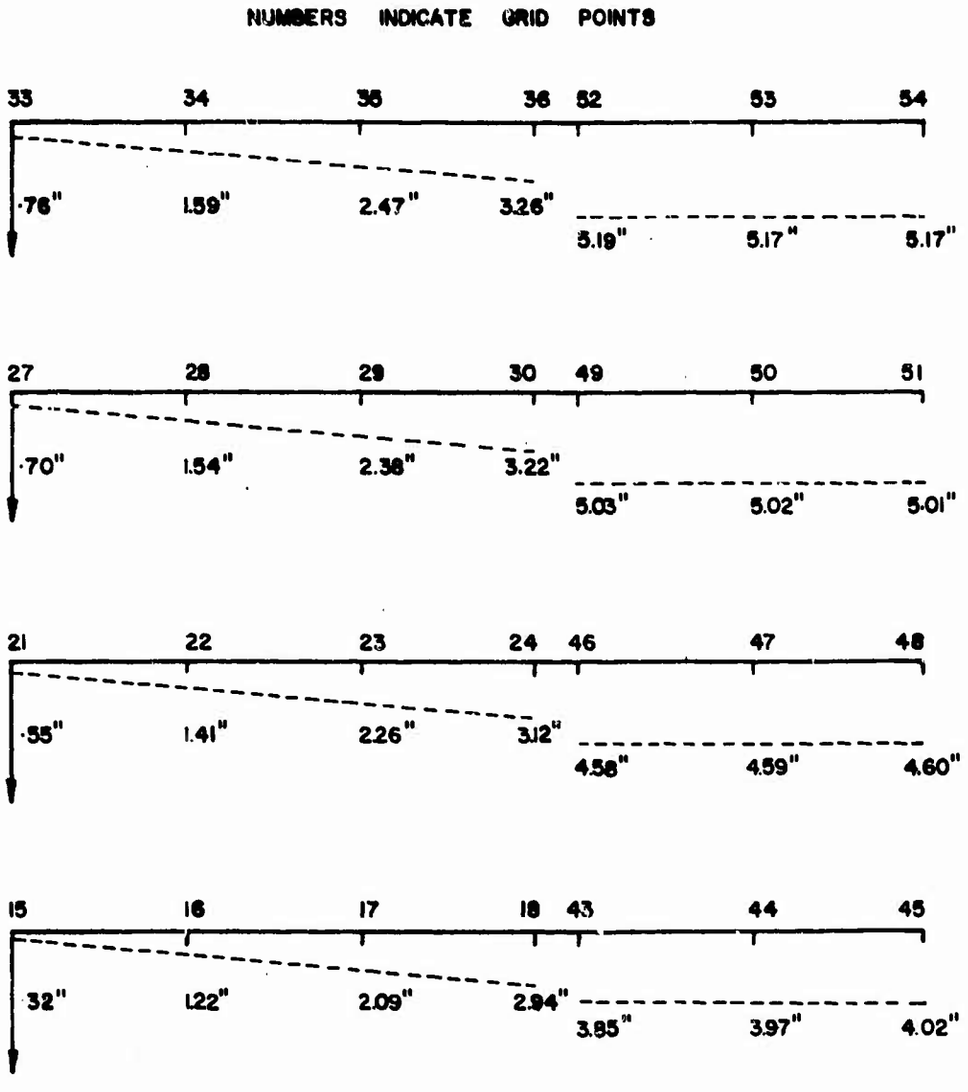
NUMBERS INDICATE GRID POINTS
33
34
35
36
52
53
54
.76"
1.59"
2.47"
3.26"
5.19"
5.17"
5.17"
27
28
29
30
49
50
51
.70"
1.54"
2.38"
3.22"
5.03"
5.02"
5.01"
21
22
23
24
46
47
48
.55"
1.41"
2.26"
3.12"
4.58"
4.59"
4.60"
15
16
17
18
43
44
45
.32"
1.22"
2.09"
2.94"
3.85"
3.97"
4.02"

Fig. 19 (Cont'd)

and then adjusted from these initial values to bring computed and measured deflections under static loading into satisfactory agreement. With a concentrated load at the midpoint of the platform the maximum difference between computed and measured deflections was 7% for the Type II platform and 11% for the Type IV platform. The differences are larger at points 19, 20, 21 and 32 in the Type II platform. However the measured deflections at those points are not considered reliable because they are so small. An error of 0.001 in. represents a large percentage of the total whereas at points such as the center of the platform it is an insignificant percentage of the total. In view of the anisotropic nature of the platforms and the fact that the network of beams could only approximate the behavior of platform the agreement reached is considered satisfactory.

Calculations of moments and stresses in the Type II platform with a distributed static load of 106.1 lb/ft^2 and a ball support at a point 12.75 in. from the end of the platform indicate a bending stress at the center of the platform, perpendicular to the side rails, of 6230 psi, and in the direction parallel to the side rails, 865 psi. Deflection at the center is 1.89 in. Moving the support closer to the end of the platform increases the stresses and deflections, and vice versa, moving the support farther from the end decreases the stress.

For the dynamic loading of this platform with the sling attached at a point 12.75 in. from the end of the platform (point 3) the maximum deflection at the center is 5.17 in. This maximum occurs 1.2 seconds after the action of main parachute starts. The stresses at the center of the platform when the maximum deflection occurs are 1010 psi parallel to the side rail and 24,500 psi perpendicular to the side rail.

For the Type IV platform under a distributed static loading of 1000 lb the deflection shape is almost cylindrical. The maximum bending moment in each spreader occurs at the center and the maxima are essentially the same for each spreader. The maximum stress is 285 psi. Deflection at the center of the platform is 0.32 in. In the side rail the maximum bending stress is 2880 psi. Dynamic loading of the Type IV platform has not been investigated.

4. Conclusions

a. Both the Type II and Type IV platforms can be satisfactorily represented for computational purposes by

an irregular network of beams rigidly attached to each other at the cross over points.

b. The Jet Propulsion Stiff-Eig computer program is satisfactory for static load computations.

c. The influence coefficent method, and the Runge-Kutta-Gill computational scheme for computing dynamic stresses and deflections is satisfactory if the mass loading, and the moment of inertia loading are about the same at each joint. However, if these quantities are zero, or very small, at any one joint that joint must be removed from the computations. This means that since distributed loads cannot be placed on the side rails the mass loadings will be small at the grid points along the rails. Therefore these must be eliminated in the computations. Consequently no information can be obtained directly concerning the maximum moments and stresses in the rails.

d. Static loading computations indicate that the critical stresses occur in the rails. This in combination with conclusion c indicates that a computational procedure which will allow the rails to be included is required.

e. The computational results for dynamic loading are believed to be reliable for the assumed conditions, but in view of the limitations referred to in (c) and in the absence of experimental data these computed results should be regarded only as an indication of the order of magnitude of the deflections of the center of the platform relative to the sling attachment point for the assumed loading.

References

1. Przemieniecki, J. S., Theory of Matrix Structural Analysis, McGraw-Hill Chapters 5 and 6 1968.

2. Batchelder, R. R. and B. K. Wada, "Stiffness Matrix Structural Analysis.," Technical Memorandum No. 33-75. Jet Propulsion Laboratory, CIT, Pasadena.

3. Timoshenko, S. P. and J. N. Goodier, Theory of Elasticity, McGraw-Hill Second Edition Chapter 11 1951.

4. Meyer, L. H., Plywood McGraw-Hill 1947.

5. Wangaard, F. F., The Mechanical Properties of Wood, John Wiley & Sons, Inc. 1950.

6. Wang, P. C., Numerical and Matrix Methods in Structural Mechanics, John Wiley & Sons, Inc. Chapters 3 and 8 1966.

7. Anderson, R. G., B. M. Irons and O. C. Zienkiewicz. "Vibration and Stability of Plates using Finite Elements," Int. J. Solids Structures, 1968, Vol. 4, pages 1031-1055 Pergamon Press.

APPENDIX A

Typical Cross Sections

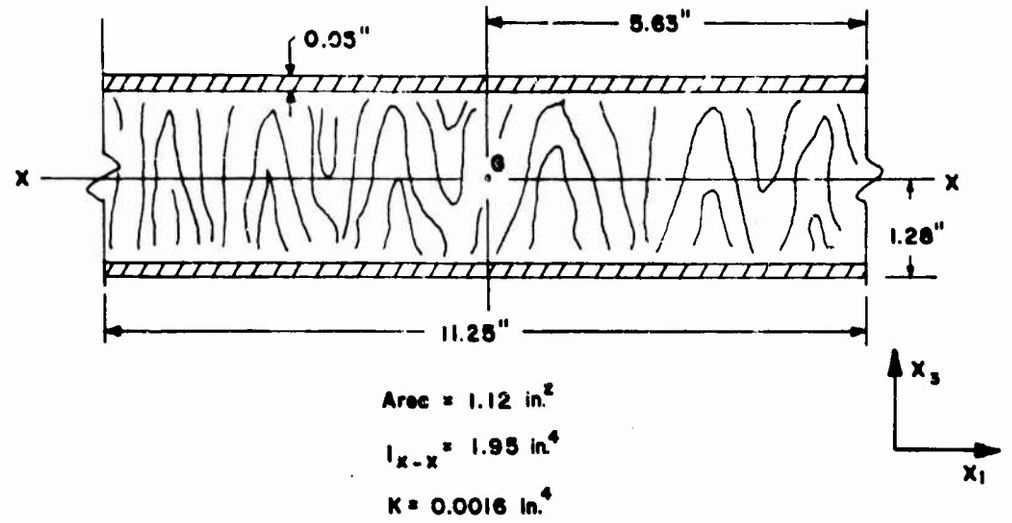

Area = 1.12 $in.^2$

I_{x-x} = 1.95 $in.^4$

K = 0.0016 $in.^4$

SECTION A - A

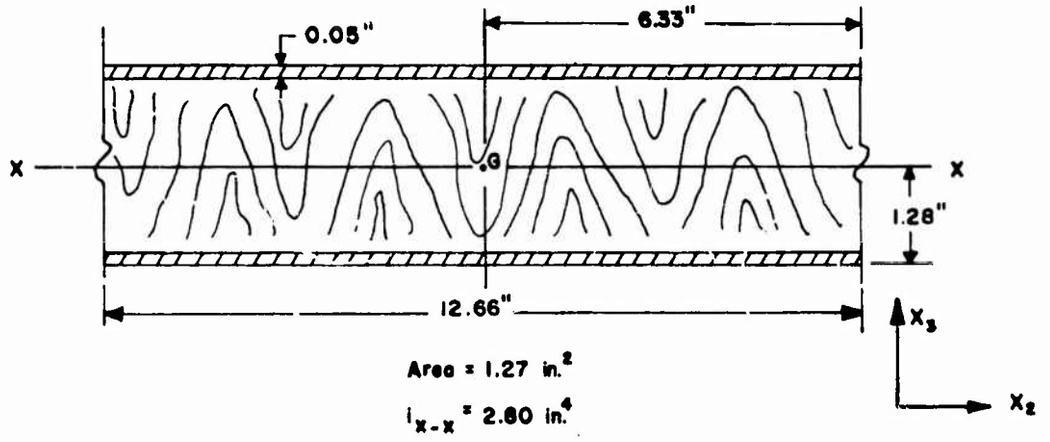

Area = 1.27 $in.^2$

I_{x-x} = 2.80 $in.^4$

K = 0.00106 $in.^4$

SECTION B - B

Fig. 1A Sections A - A and B - B of Type II Platform

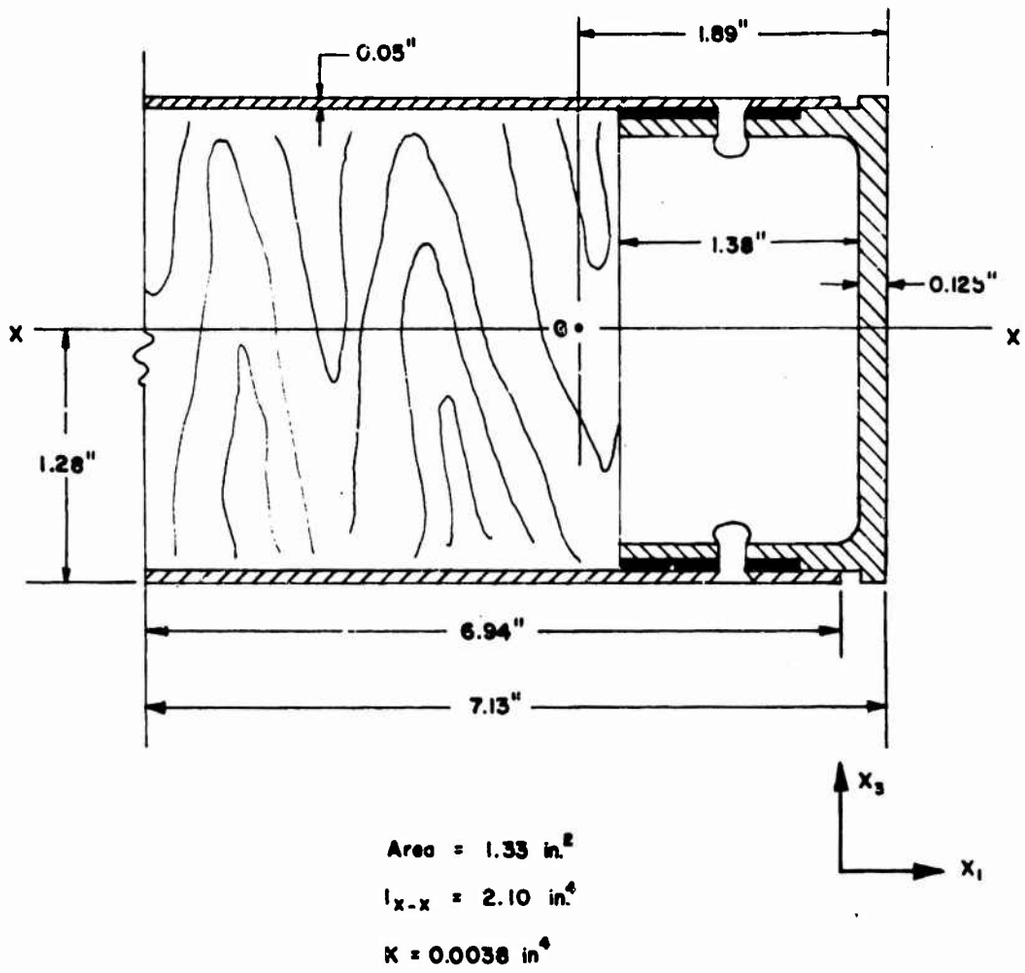

SECTION C - C

Fig. 2A Section C - C of Type II Platform

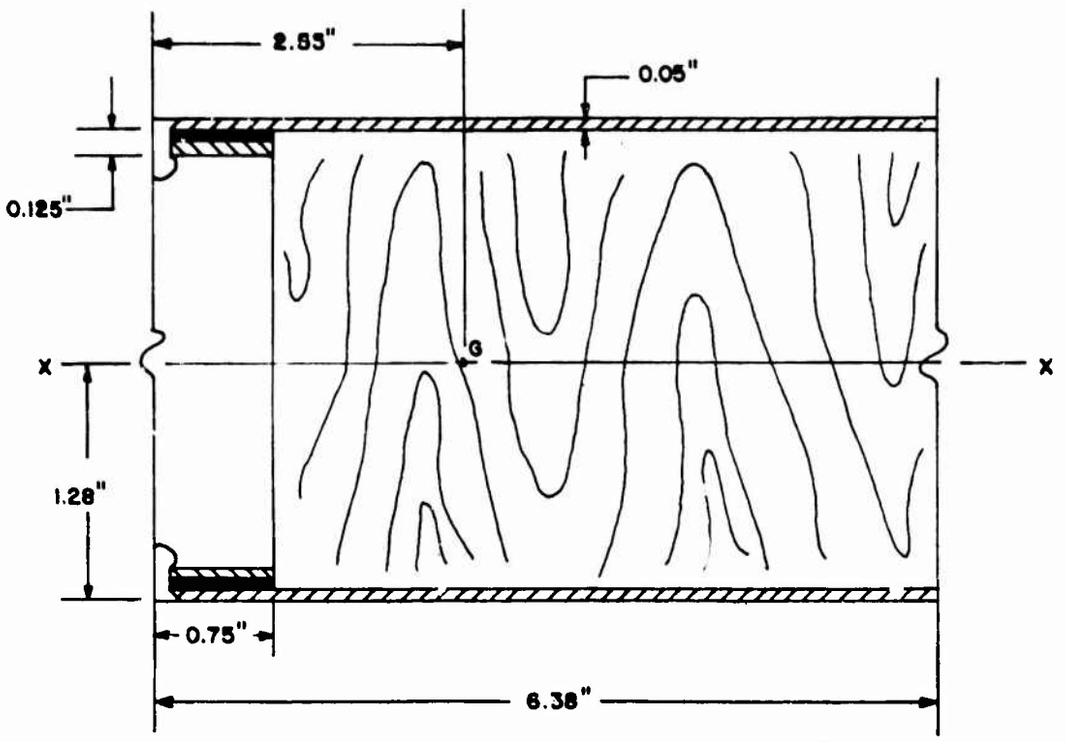

Area = 0.625 $in.^2$

I_{X-X} = 1.31 $in.^4$

K = 0.00157 $in.^4$

SECTION D – D

Fig. 3A Section D - D of Type II Platform

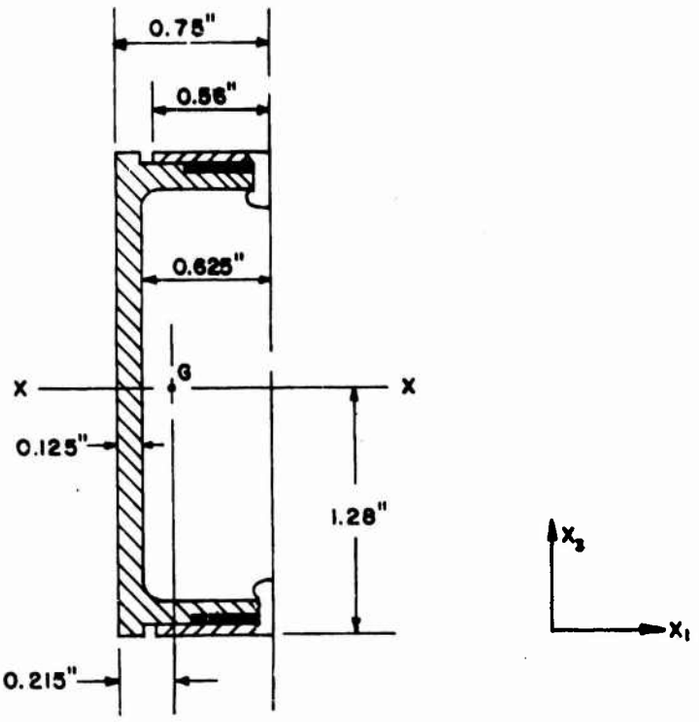

Area = 0.532 $in.^2$

I_{x-x} = 0.560 $in.^4$

K = 0.0031 $in.^4$

SECTION E - E

Fig. 4A Section E - E of Type II Platform

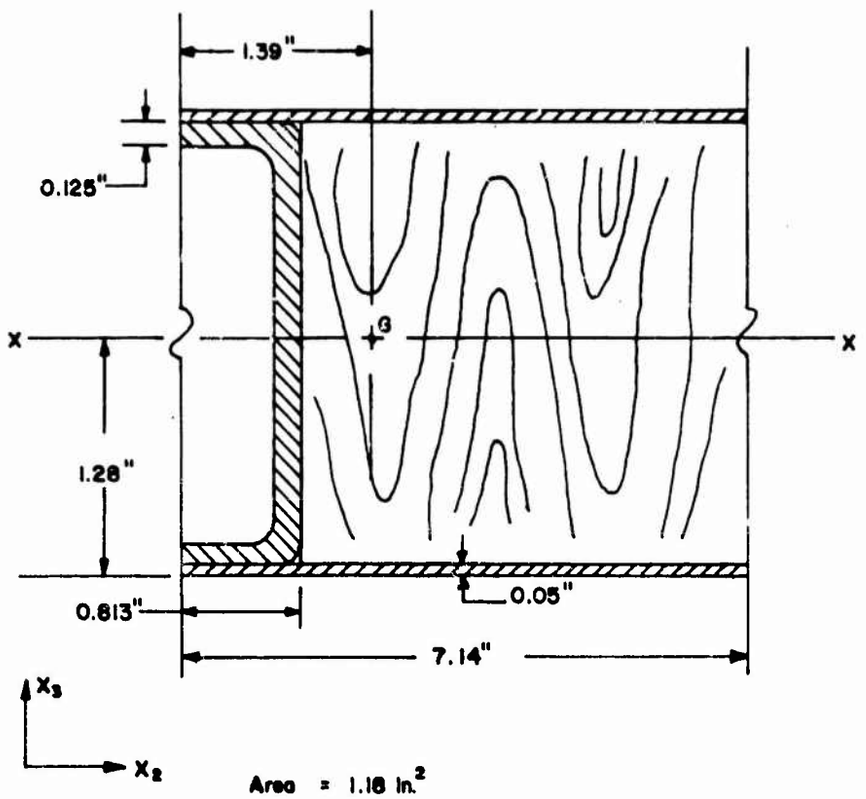

Fig. 5A Section F - F of Type II Platform

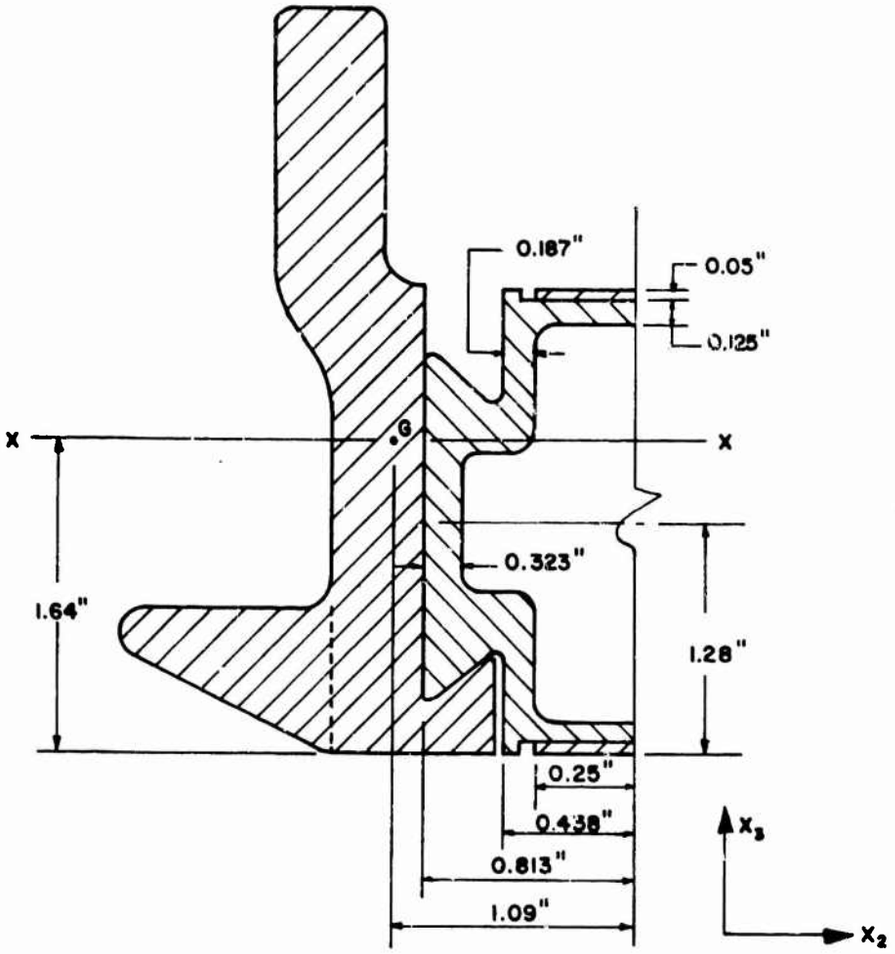

Area = 3.95 $in.^2$

I_{x-x} = 5.40 $in.^4$

K = 0.37 $in.^4$

SECTION G - G

Fig. 6A Section G - G of Type II Platform

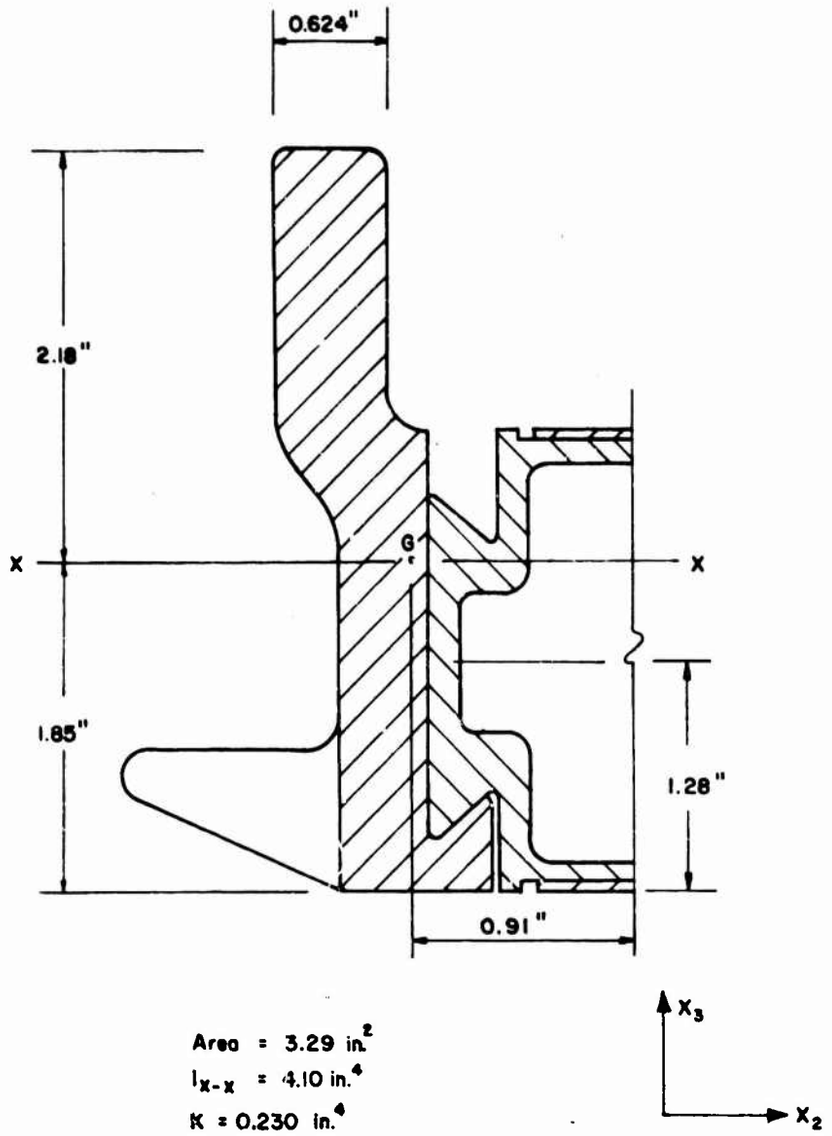

Fig. 7A Taken Through Rail Slot of Type II Platform

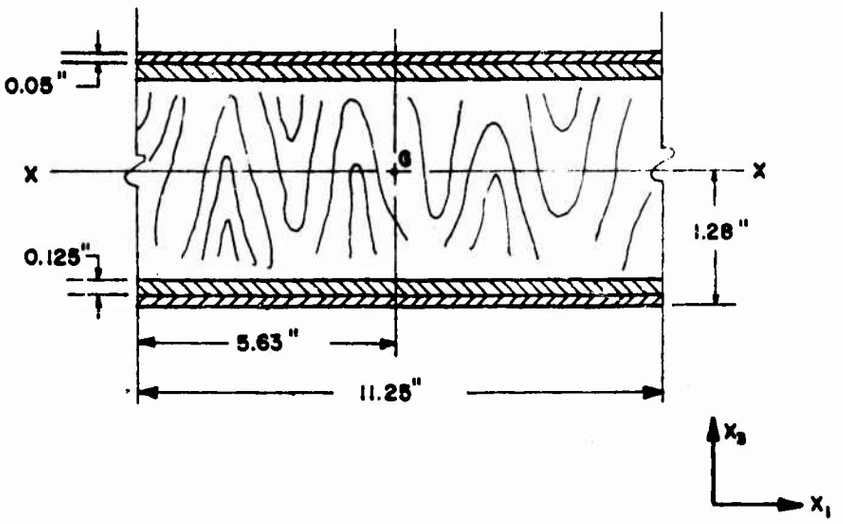

Area = 2.03 $in.^2$

I_{x-x} = 5.50 $in.^4$

K = 0.012 $in.^4$

SECTION H - H

Fig. 8A Section H - H of Type II Platform

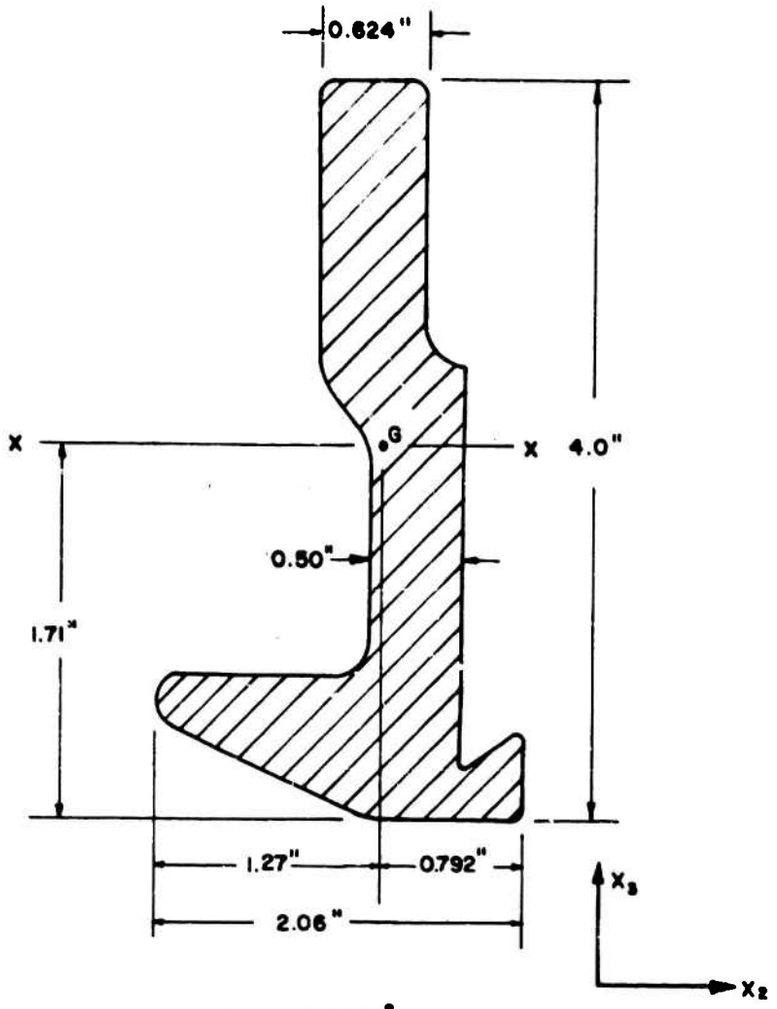

Fig. 9A Section I - I of Type II Platform

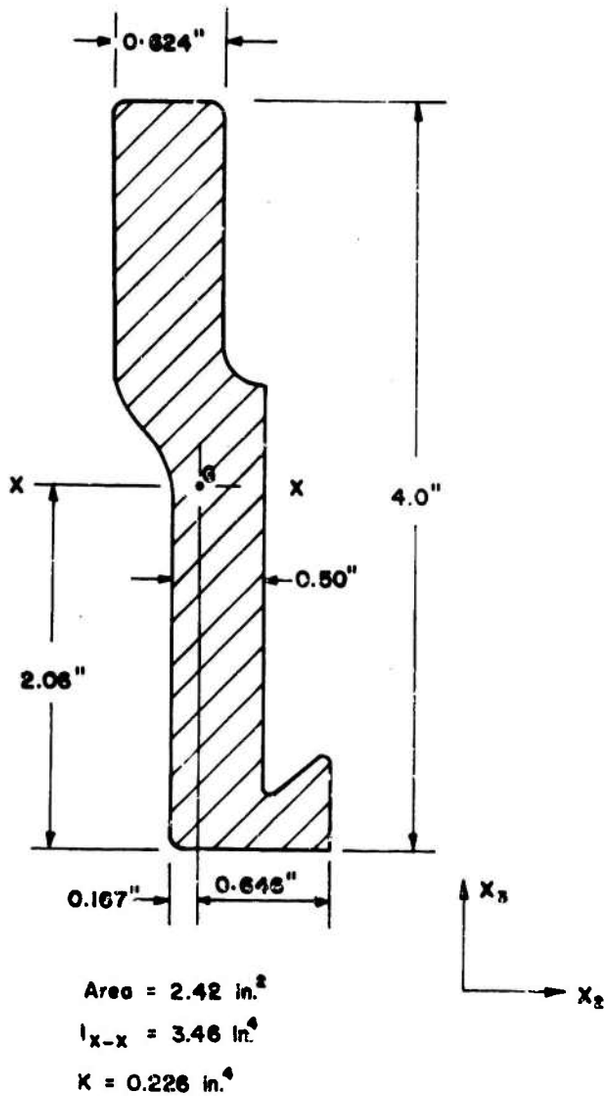

Fig. 10A Section I - I of Type II Platform Taken Through Rail Slot

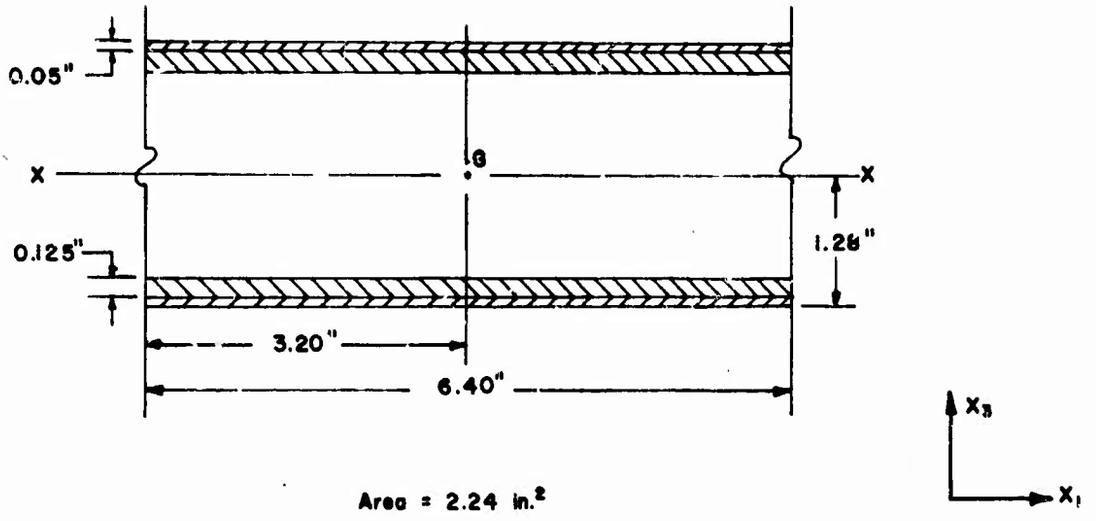

Area = 2.24 $in.^2$

I_{x-x} = 2.70 $in.^4$

K = 0.007 $in.^4$

SECTION J - J

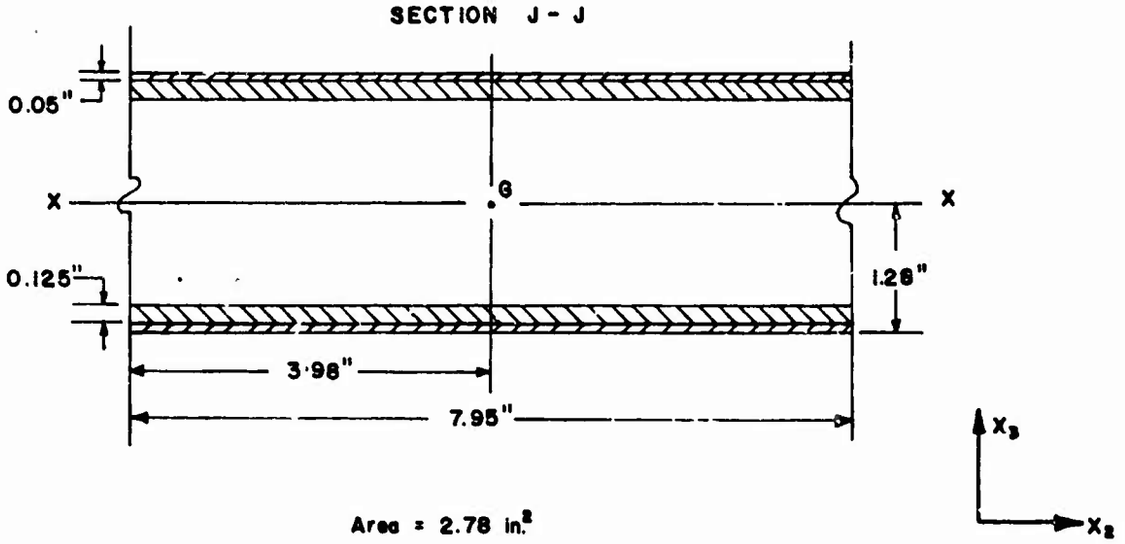

Area = 2.78 $in.^2$

I_{x-x} = 4.35 $in.^4$

K = 0.013 $in.^4$

SECTION K - K

Fig. 11A Sections J - J and K - K of Type II Platform

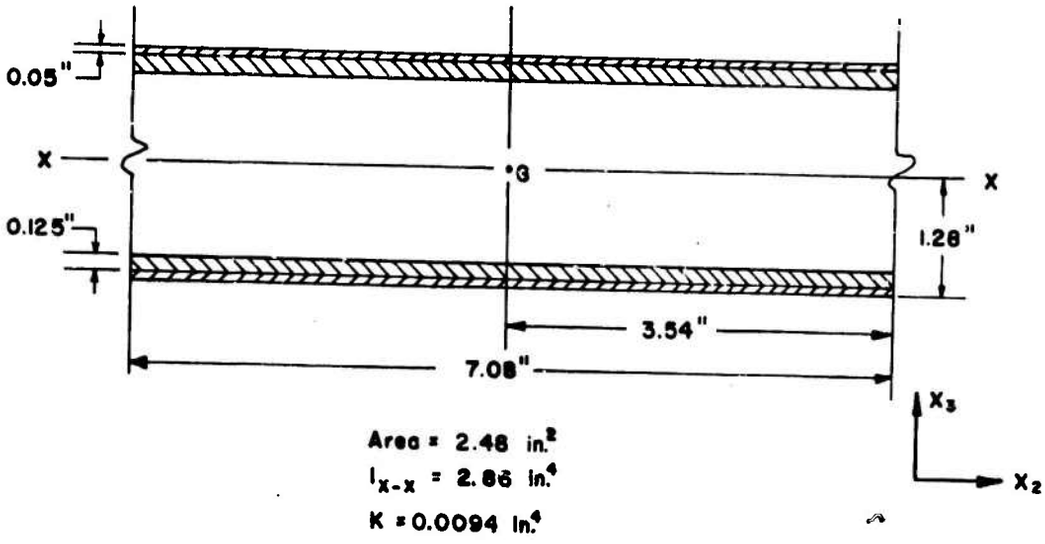

Area = 2.48 $in.^2$

I_{x-x} = 2.86 $in.^4$

K = 0.0094 $in.^4$

SECTION L - L

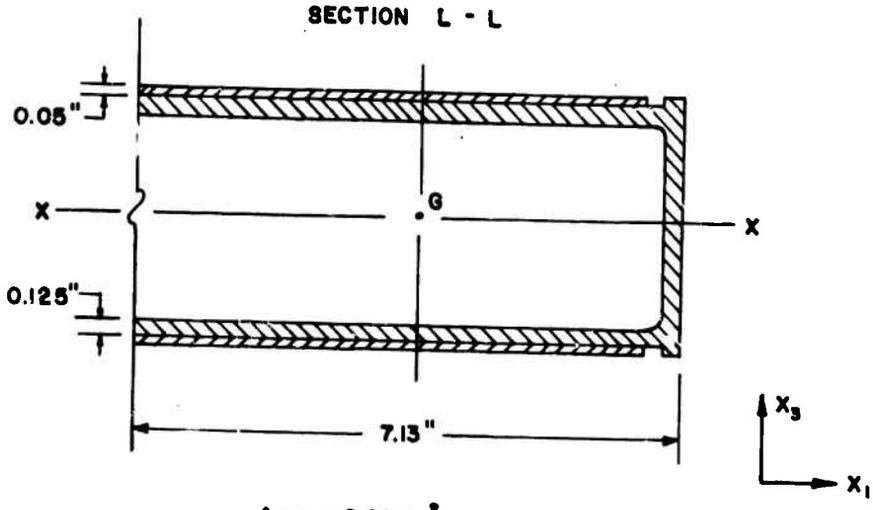

Area = 2.49 $in.^2$

I_{x-x} = 3.91 $in.^4$

K = 0.00896 $in.^4$

SECTION M - M

Fig. 12A Sections L - L and M - M of Type II Platform

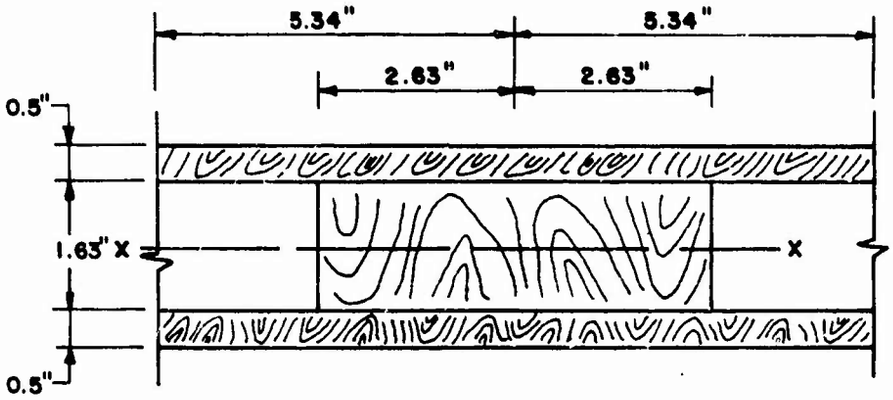

I_{x-x} = 5.00 in.^{4}

K = 2.92 in.^{4}

SECTION A - A

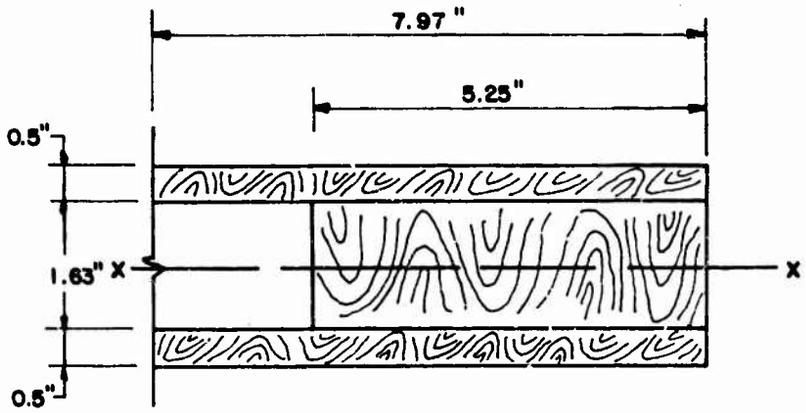

I_{x-x} = 4.40 in.^{4}

K = 2.57 in.^{4}

SECTION B - B

Fig. 13A Sections A - A and B - B of Type IV Platform

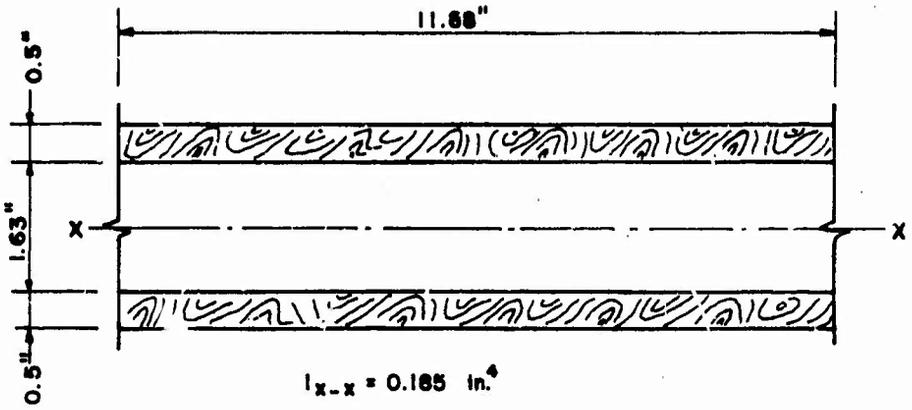

$I_{x-x} = 0.185$ in.^{4}

K = 0.018 in.^{4}

SECTION C - C

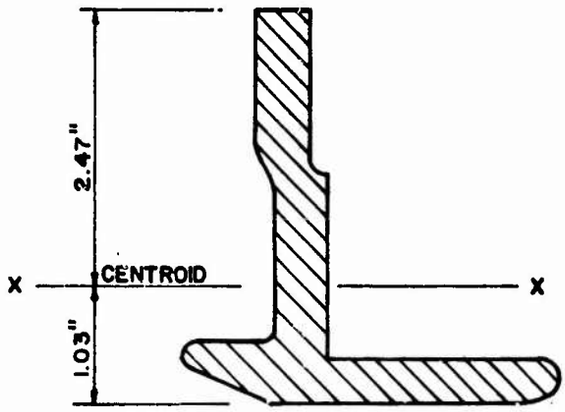

$I_{x-x} = 5.38$ in.^{4}

K = 0.085 in.^{4}

SECTION D-D

Fig. 14A Sections C - C and D - D of Type IV Platform

APPENDIX B

Tabulations of Deflections and Section Properties

TABLE IB

Type II Platform Measured and Computed Deflections
1000 lb Concentrated Load at the Center of Platform

Grid Point	Measured-Inches	Calculated-Inches
2	0.000	0.000
4	-0.226	-0.219
6	-0.406	-0.394
9	-0.107	-0.112
11	-0.314	-0.316
15	-0.106	-0.111
17	-0.311	-0.319
19	0.010	0.012
20	0.006	-0.002
22	-0.208	-0.217
24	-0.412	-0.433
27	-0.102	-0.110
29	-0.309	-0.328
31	0.008	0.014
32	-0.005	-0.001
33	-0.106	-0.110
34	-0.209	-0.219
35	-0.311	-0.330
36	-0.414	-0.441
37	-0.417	-0.410
38	-0.453	-0.449
39	-0.464	-0.461
41	-0.459	-0.457
43	-0.526	-0.510
44	-0.535	-0.522
46	-0.600	-0.581
48	-0.609	-0.585
49	-0.664	-0.627
50	-0.672	-0.631
52	-0.674	-0.642
53	-0.676	-0.649
54	-0.686	-0.654

Table IIB

Type IV Platform Measured and Computed Deflections
500 lb Concentrated Load at the Center of Platform

Grid Point	Measured-Inches	Calculated-Inches
3	0.038	0.040
4	0.039	0.039
5	0.040	0.038
6	0.041	0.038
10	-0.003	-0.003
12	-0.003	-0.005
13	-0.040	-0.041
15	-0.042	-0.044
16	-0.045	-0.046
17	-0.046	-0.047
18	-0.047	-0.047
19	-0.077	-0.079
22	-0.090	-0.088
23	-0.093	-0.089
27	-0.127	-0.123
28	-0.136	-0.128
29	-0.140	-0.130
31	-0.120	-0.124
33	-0.231	-0.229
34	-0.316	-0.293
36	-0.395	-0.351
37	-0.138	-0.142
40	-0.362	-0.363
42	-0.445	-0.442
43	-0.144	-0.149
45	-0.271	-0.301
46	-0.371	-0.401
47	-0.464	-0.477
48	-0.496	-0.510

TABLE IIIB

Type II Platform Member Stiffness Properties

Member Joint-Joint		I ($In.^4$)	K ($in.^4$)	Member Joint-Joint		I ($in.^4$)	K ($in.^4$)
1	2	4.45	o.25	49	50	2.80	o.0011
2	3	5.40	0.37	50	51	"	"
3	4	4.87	0.28	52	53	1.40	0.0005
4	5	"	"	53	54	"	"
5	6	4.10	0.23	1	7	0.52	0.0026
7	8	2.86	0.0094	7	13	0.56	0.0031
8	9	1.48	0.0028	13	19	"	"
9	10	"	"	19	25	"	"
10	11	"	"	25	31	"	"
11	12	"	"	2	8	2.70	0.007
13	14	4.35	0.013	8	14	1.31	0.0016
14	15	2.80	0.0011	14	20	"	"
15	16	"	"	20	26	"	"
16	17	"	"	26	32	"	"
17	18	"	"	3	9	5.50	0.012
19	20	4.35	0.013	9	15	1.95	0.0016
20	21	2.80	0.0011	15	21	"	"
21	22	"	"	21	27	"	"
22	23	"	"	27	33	"	"
23	24	"	"	4	10	5,50	0.012
25	26	4.35	0.013	10	16	1.95	0.0016
26	27	2.80	0.0011	16	22	"	"
27	28	"	"	22	28	"	"
28	29	"	"	28	34	"	"
29	30	"	"	5	11	5.50	0.012
31	32	2.18	0.0065	11	17	1.95	0.0016
32	33	1.40	0.0005	17	23	"	"
33	34	"	"	23	29	"	"
34	35	"	"	29	35	"	"
35	36	"	"	6	12	3.91	0.010
37	38	4.10	0.19	12	18	2.10	0.0038
38	39	4.90	0.29	18	24	"	"
40	41	1.48	0.0028	24	30	"	"
41	42	"	"	30	36	"	"
43	44	2.80	0.0011	37	40	3.91	0.010
44	45	"	"	40	43	2.10	0.0038
46	47	"	"	43	46	"	"
47	48	"	"	46	49	"	"

TABLE III B (Cont'd)

Type II Platform Member Stiffness Properties

Member Joint-Joint		I ($in.^4$)	K ($in.^4$)
49	52	2.10	0.0038
38	41	5.50	0.012
41	44	1.95	0.0016
44	47	"	"
47	50	"	"
50	53	"	"
39	42	2.75	0.0060
42	45	0.975	0.0008
45	48	"	"
48	51	"	"
51	54	"	"
6	37	5.20	0.130
12	40*	0	0
18	43*	0	0
24	46*	0	0
30	49*	0	0
36	52*	0	0

*Discontinuity Members
$I = K = 0.000001$ $in.^4$ was used in the calculation of deflection.

TABLE IVB

Type IV Platform Member Stiffness Properties

Member Joint-Joint		I_4 (in.^{4})	K_4 (in.^{4})	Member Joint-Joint		I_4 (in.^{4})	K_4 (in.^{4})
1	2	4.40	2.57	47	47	2.50	1.46
2	3	"	"	1	7	5.38	0.065
3	4	"	"	7	13	"	"
4	5	"	"	13	19	"	"
5	6	"	"	19	25	"	"
7	8	5.00	2.92	25	31	"	"
8	9	"	"	31	37	"	"
9	10	"	"	37	43	"	"
10	11	"	"	2	8	0.185	0.018
11	12	"	"	8	14	"	"
13	14	"	"	14	20	"	"
14	15	"	"	20	26	"	"
15	16	"	"	26	32*	0	0
16	17	"	"	32	38	0.185	0.018
17	18	"	"	38	44	"	"
19	20	"	"	3	9	"	"
20	21	"	"	9	15	"	"
21	22	"	"	15	21	"	"
22	23	"	"	21	27	"	"
23	24	"	"	27	33*	0	0
25	26	4.40	2.57	33	39	0.185	0.018
26	27	"	"	39	45	"	"
27	28	"	"	4	10	"	"
28	29	"	"	10	16	"	"
29	30	"	"	16	22	"	"
31	32	"	"	22	28	"	"
32	33	"	"	28	34*	0	0
33	34	"	"	34	40	0.185	0.018
34	35	"	"	40	46	"	"
35	36	"	"	5	11	"	"
37	38	5.00	2.92	11	17	"	"
38	39	"	"	17	23	"	"
39	40	"	"	23	29	"	"
40	41	"	"	29	35*	0	0
41	42	"	"	35	41	0.185	0.018
43	44	2.50	1.46	41	47	"	"
44	45	"	"	6	12	0.093	0.0096
45	46	"	"	12	18	"	"
46	47	"	"	18	24	"	"

TABLE IVB (Cont'd)

Type IV Platform Member Stiffness Properties

Member Joint--Joint		I ($in.^4$)	K ($in.^4$)
24	30	0.093	0.0096
30	36*	0	0
36	42	0.093	0.0096
42	48	"	"

*Discontinuity Members
$I = K = 0.000001\ in.^4$ was used in the calculation of deflection.

APPENDIX C

Deflections and Moments for a Type II Platform Statically Loaded with a Uniform Load of 106.1 Lb/Ft^2

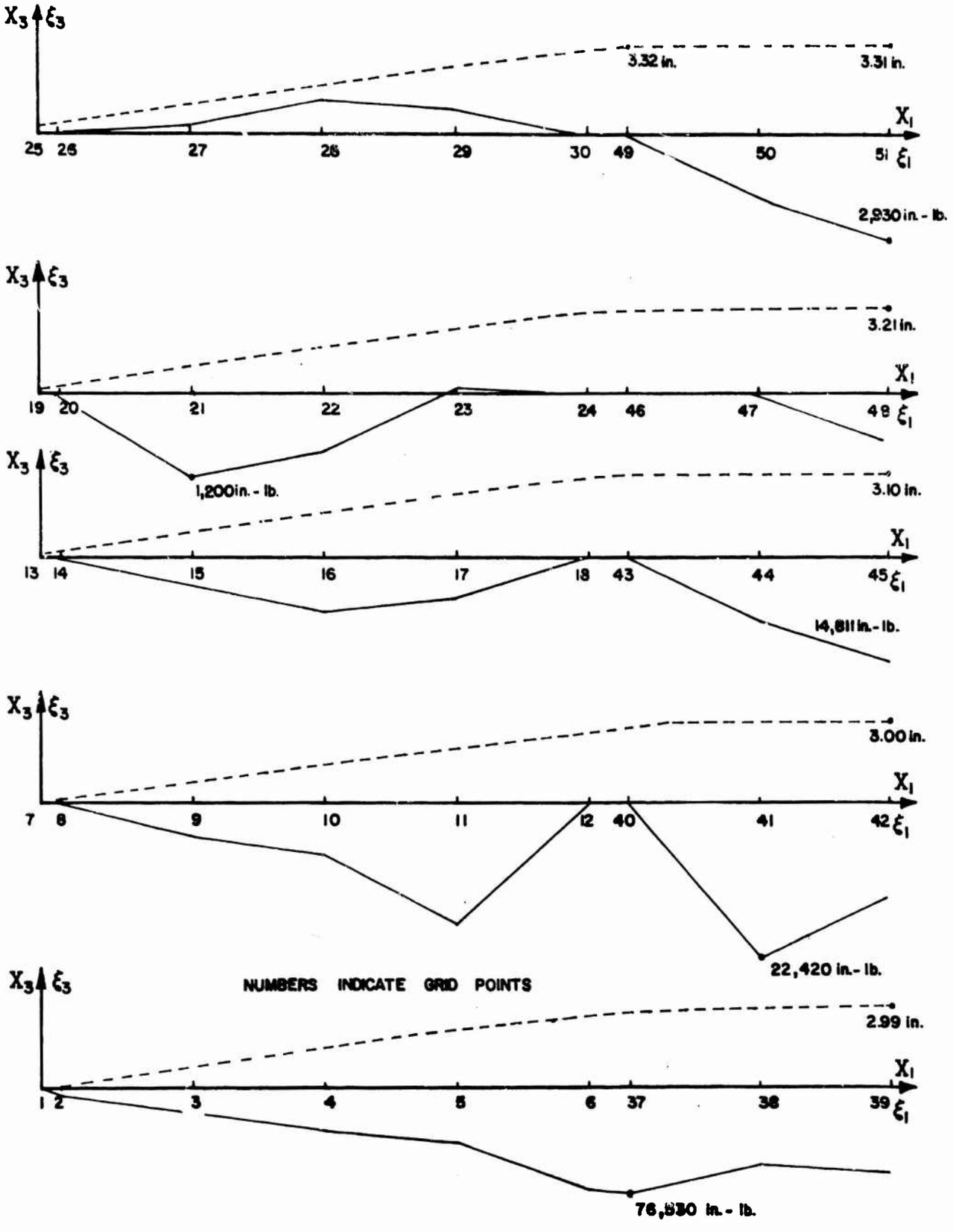

Fig. 1C Bending Moments and Deflections of Type II Platform with Support at Point 2.

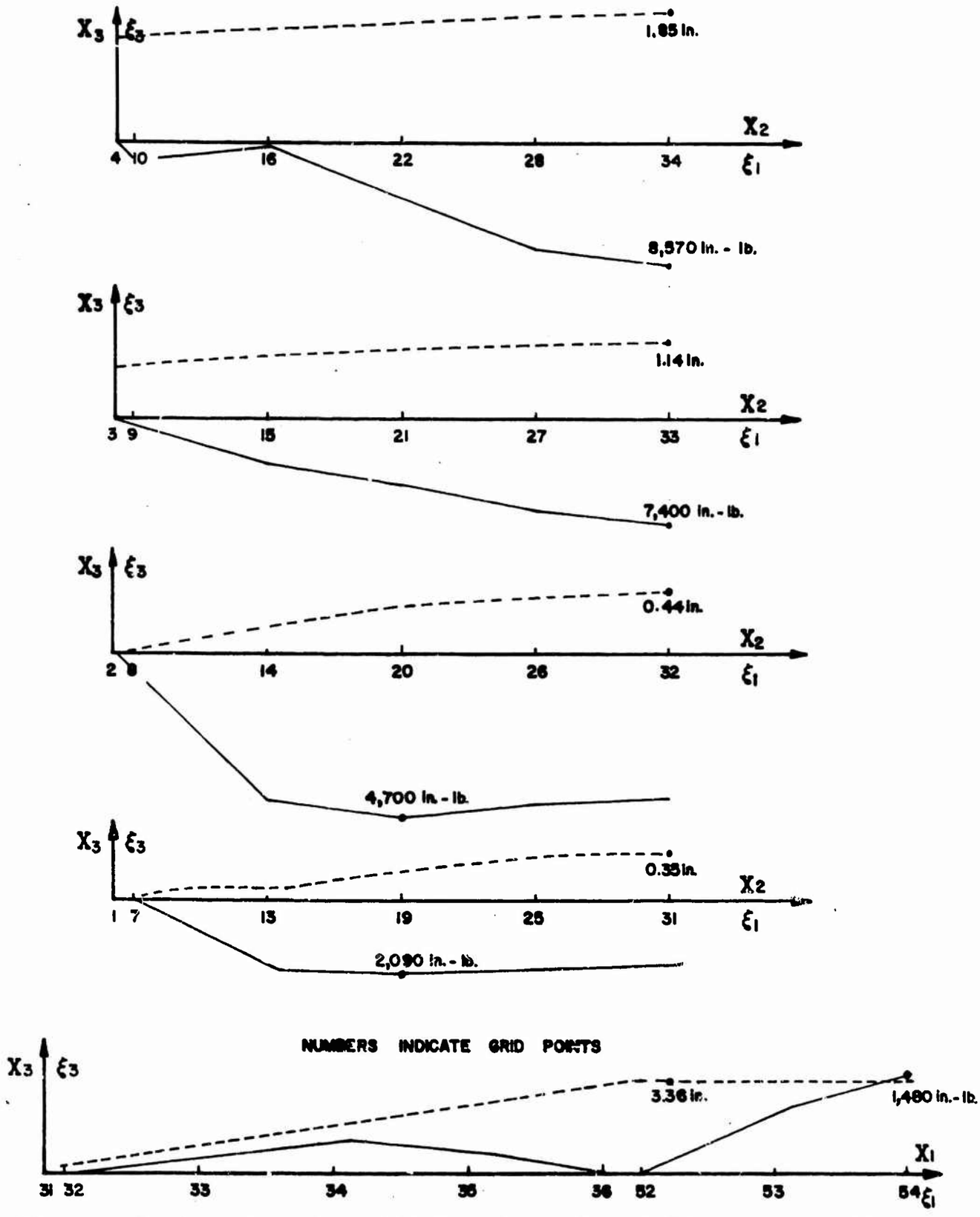

Fig. 2C Bending Moments and Deflections of Type II Platform with Support at Point 2.

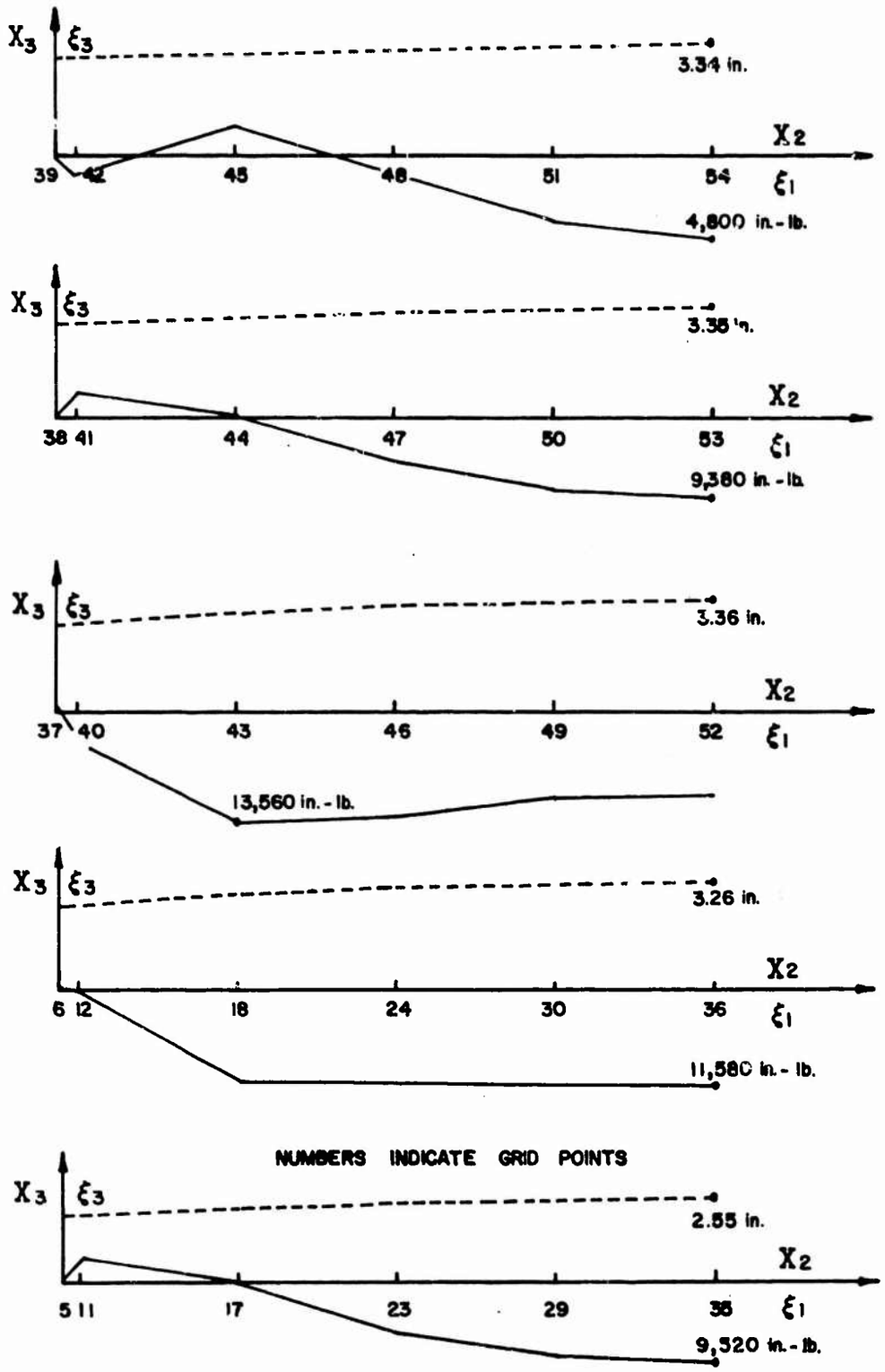

Fig. 3C Bending Moments and Deflections of Type II Platform with Support at Point 2

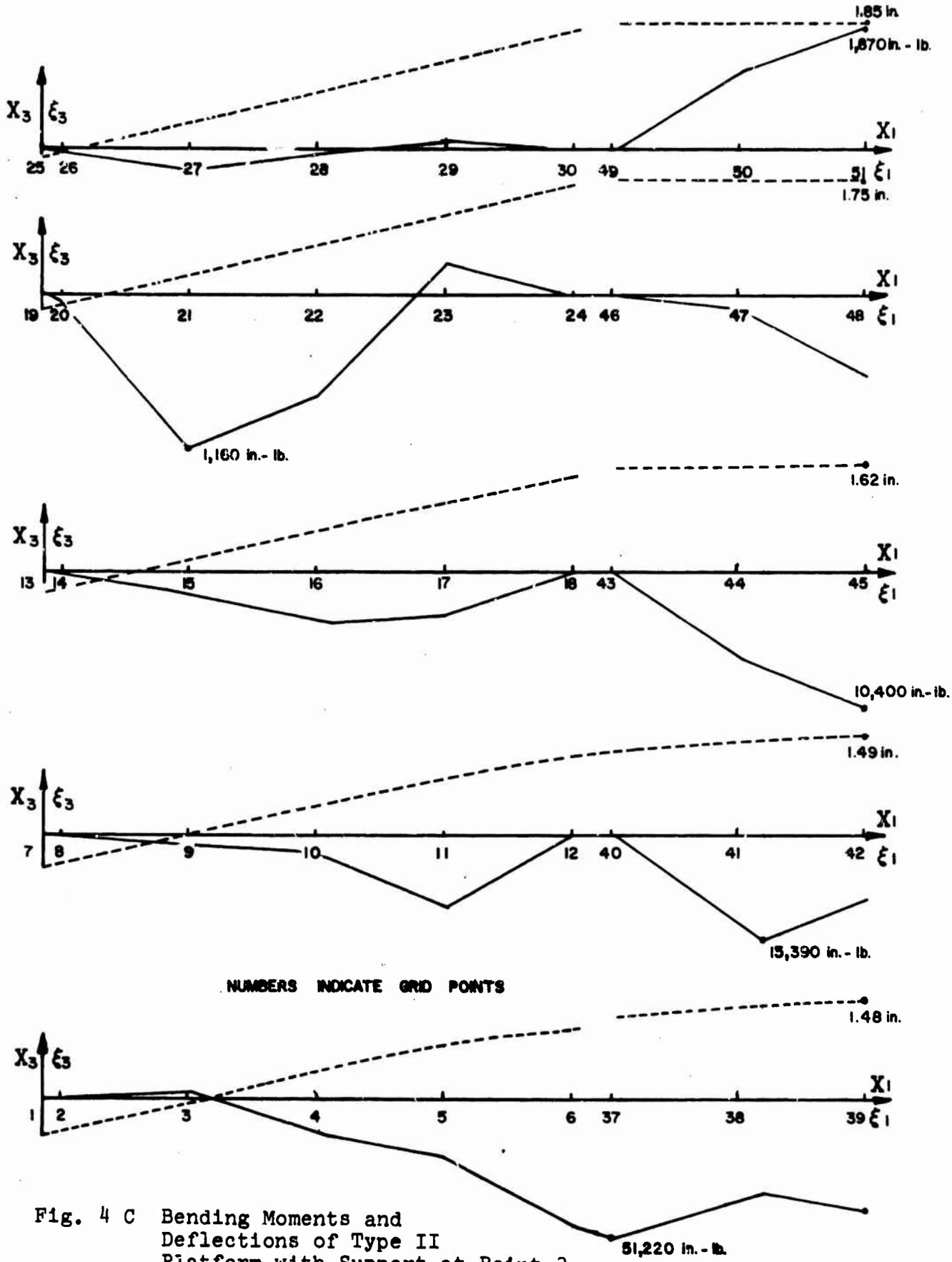

Fig. 4 C Bending Moments and Deflections of Type II Platform with Support at Point 3.

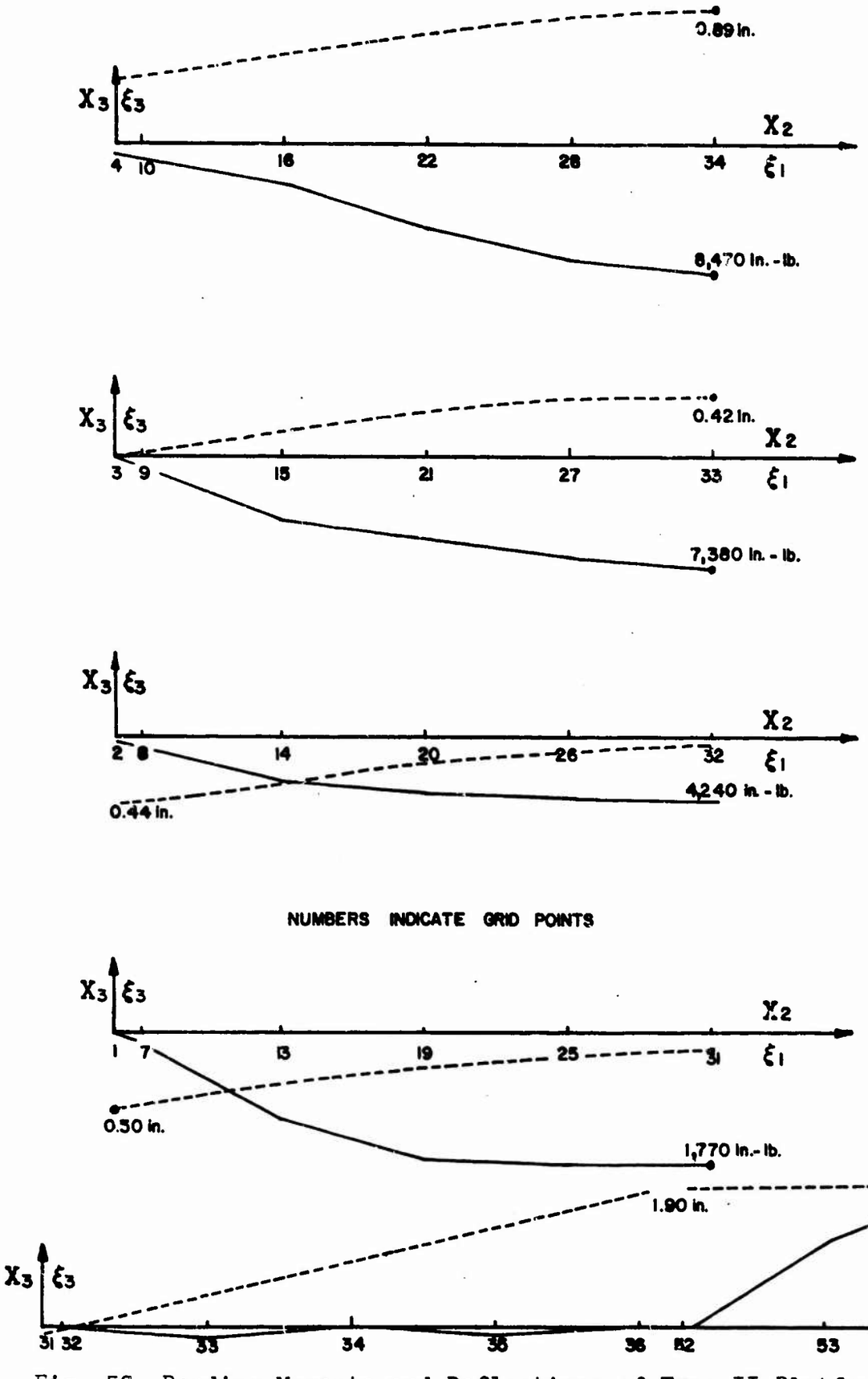

Fig. 5C Bending Moments and Deflections of Type II Platform with Support at Point 3.

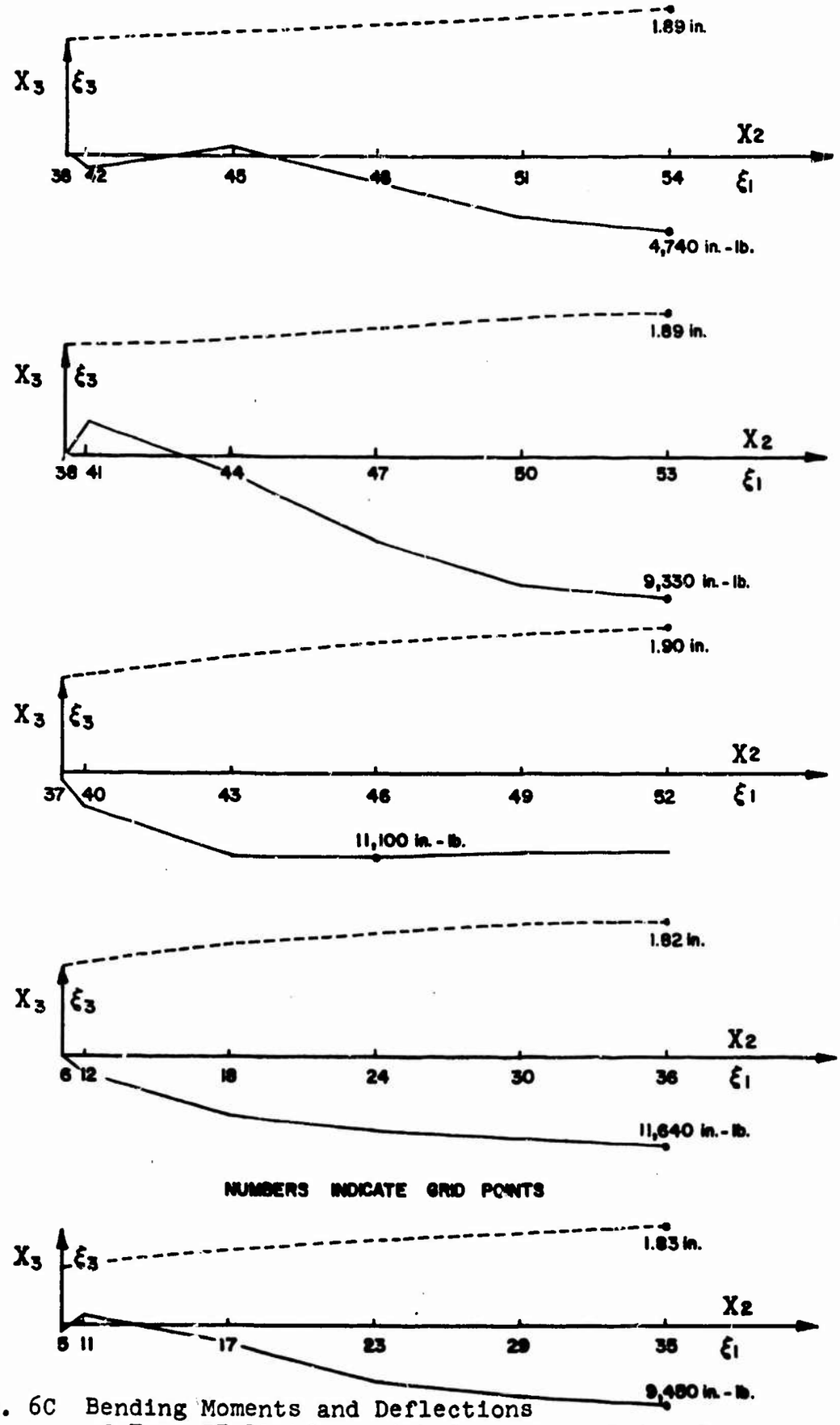

Fig. 6C Bending Moments and Deflections of Type II Platform with Support at Point 3.

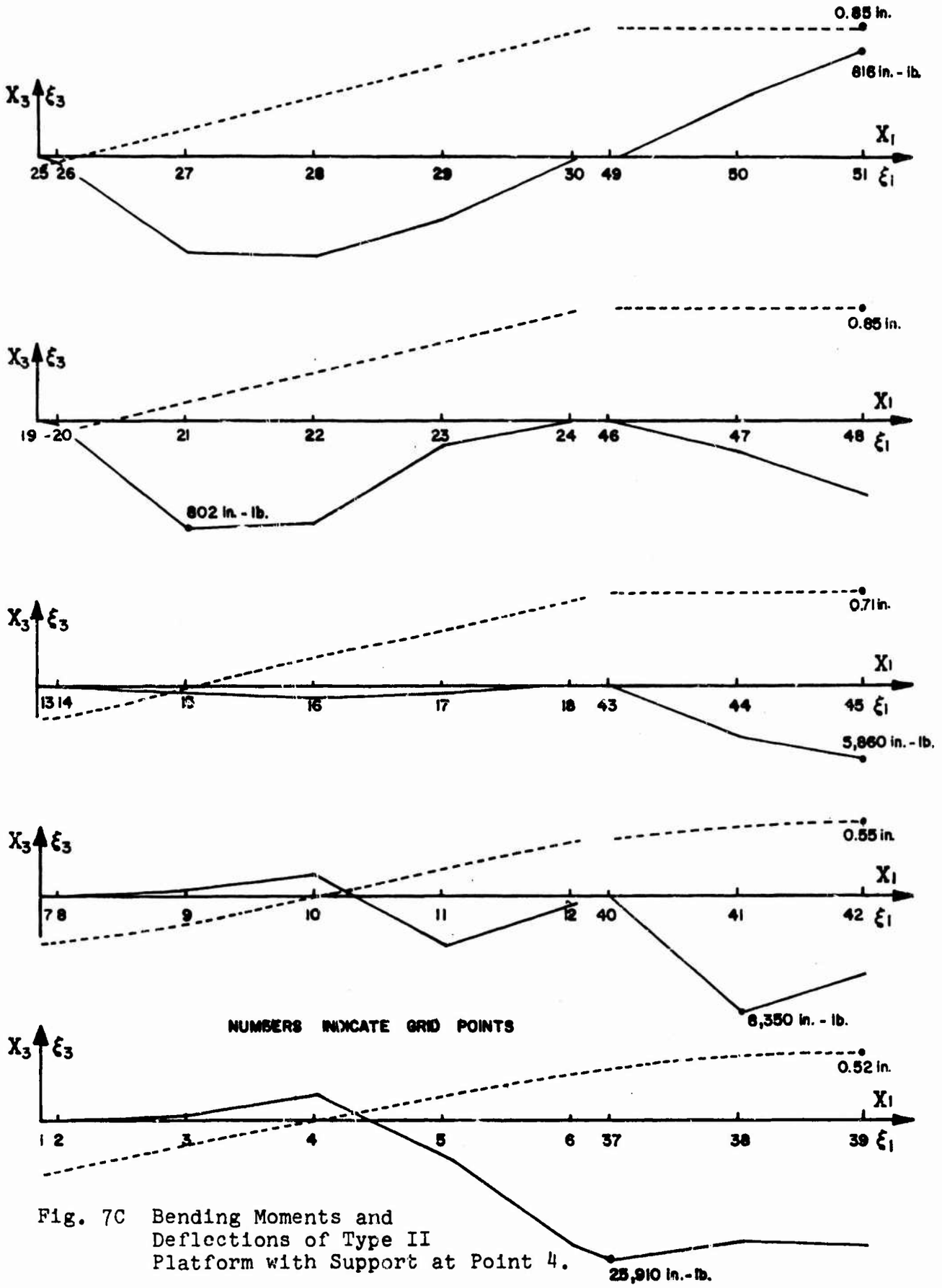

Fig. 7C Bending Moments and Deflections of Type II Platform with Support at Point 4.

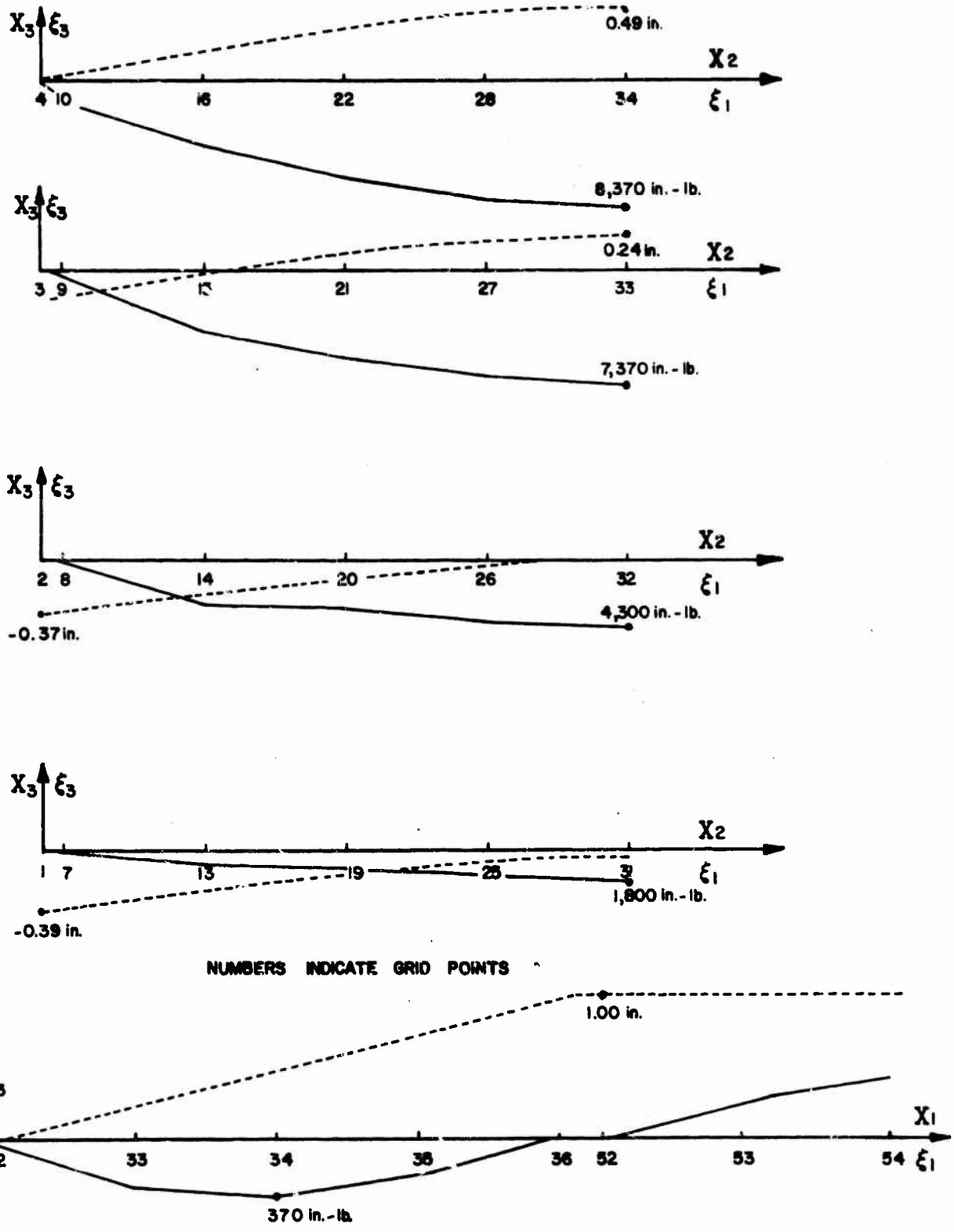

Fig. 8C Bending Moments and Deflections of Type II Platform with Support at Point 4.

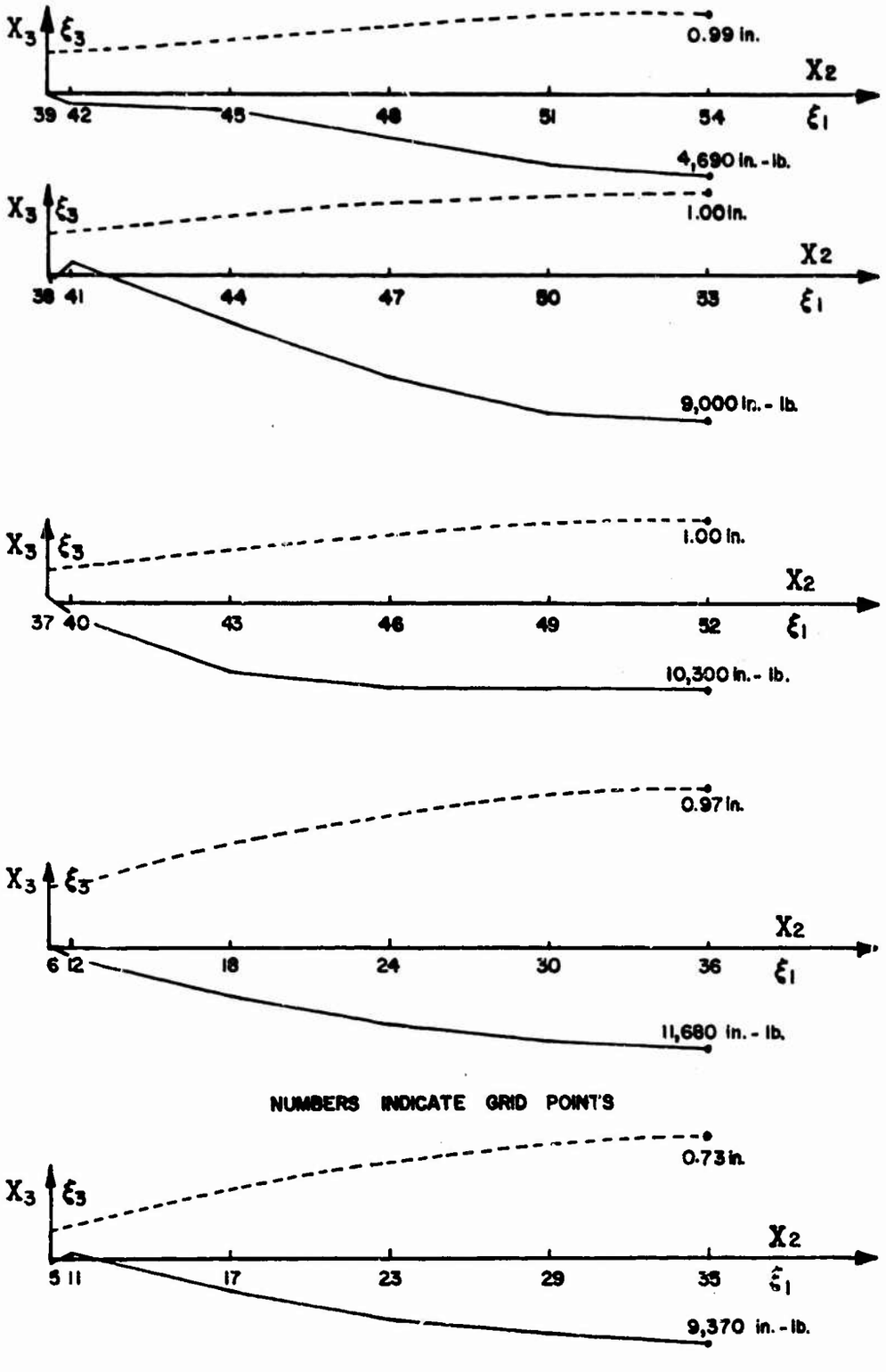

Fig. 9C Bending Moments and Deflections of Type II Platform with Support at Point 4.

APPENDIX D

Computer Programs for Analysis of Dynamic Response

Flow Chart for the Program which Generates the Stiffness Matrix of the Grid

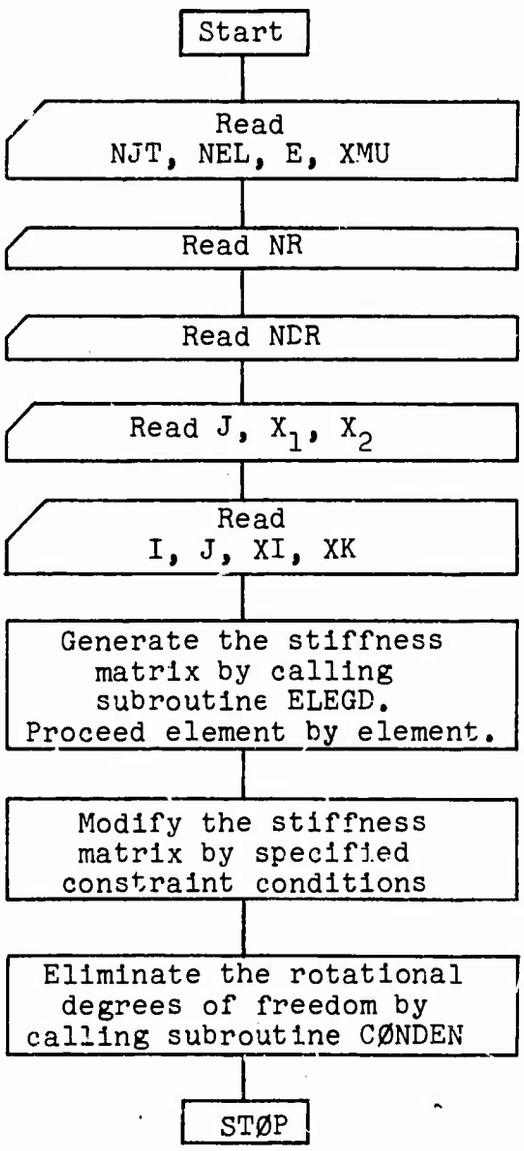

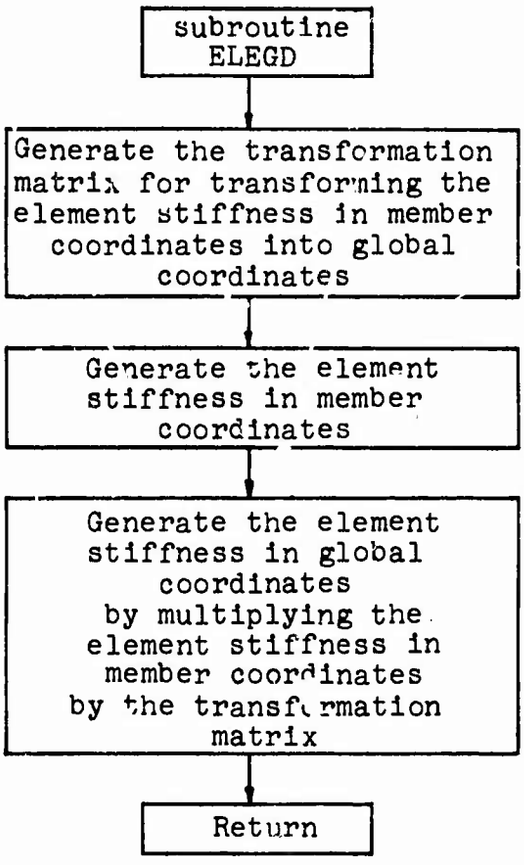
subroutine ELEGD
Generate the transformation matrix for transforming the element stiffness in member coordinates into global coordinates
Generate the element stiffness in member coordinates
Generate the element stiffness in global coordinates by multiplying the element stiffness in member coordinates by the transformation matrix
Return

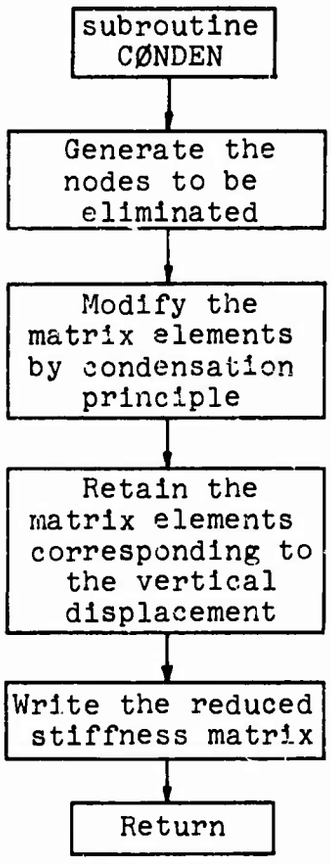
subroutine CØNDEN
Generate the nodes to be eliminated
Modify the matrix elements by condensation principle
Retain the matrix elements corresponding to the vertical displacement
Write the reduced stiffness matrix
Return

Input Sequence for the Program which Generates the Stiffness Matrix of the Grid

1. NJT, NEL, E, XMU
   Format (2I8, 7F8.4)
   NJT: number of joints in the grid.
   NEL: number of elements in the grid.
   E: Modulus of Elasticity for all elements (10^6 psi).
   XMU: Poisson's ratio for all elements.

2. NR
   Format (I8)
   NR: number of degrees of freedom to be restrained.
   Fully constrained joint has 3 degrees of freedom restrained while partially constrained joint may have 1 or 2 degrees of freedom restrained.
   If there is no constraint in the grid, NR = 0.

3. NDR (M), M = 1, NR
   Format (10I8)
   NDR: degrees of freedom constrained.
   For example: If joint 2 and joint 4 have been fully constrained, then NR = 2 x 3 = 6, NDR = 4, 5, 6, 10, 11, 12.

4. J, NDUM, (X (I,K), K = 1, 2)
   Format (2I8, 7F8.4)
   J: joint number.
   NDUM: Dummy, leave blank.
   X: joint coordinates (X_1, X_2).
   Note: joint number J should be started from 1 and then 2, 3, ... in order. Each card includes joint J, blank, coordinates X_1 and X_2.

5. I, J, XI, XK
   Format (2I8, 7F8.4)
   I, J are joint numbers of an element.
   XI: moment of inertia of the element.
   XK: torsional constant of the element.

```
C       GENERATION OF STIFFNESS MATRIX OF THE GRID
C       ALL THE ROTATIONAL DEGREES OF FREEDOM ARE REDUCED.
C       CDC 6600 ,  FORTRAN IV , STORAGE REQUIRED  50000 WORDS
        DIMENSION X1(15),X2(15),NDR(30)
        DIMENSION X(60,2),EKG(6,6),ST(170,170)
        COMMON X,EKG
100     FORMAT (1H1)
101     FORMAT (2I8,7F8.4)
102     FORMAT (1X,* ERROR, JOINT NO. NOT IN ORDER *)
103     FORMAT (1X,I3,1X,10E13.5,/(5X,10E13.5))
104     FORMAT (1X,*NO. OF JT, NO. OF ELE, E AND POIS *)
105     FORMAT (1X,* GRID COORD. *)
106     FORMAT (1X,* ELEMENT PROPERTIES, I, J, XI, XK *)
107     FORMAT (1X,* NODE RESTRAINED *)
108     FORMAT (6E13.6)
201     FORMAT (10I8)
202     FORMAT (1X,* NR=    *, I3)
        READ (5,101) NJT,NEL,E,XMU
        WRITE (6,100)
        WRITE (6,104)
        WRITE (6,101) NJT,NEL,E,XMU
        READ (5,201) NR
        WRITE (6,107)
        WRITE (6,202) NR
        IF (NR.EQ.0) GO TO 31
        READ (5,201) (NDR(M),M=1,NR)
        WRITE (6,201) (NDR(M),M=1,NR)
31      CONTINUE
        WRITE (6,105)
        E=1000000.0*E
        DO 10 I=1,NJT
        READ (5,101) J,NDUM, (X(I,K),K=1,2)
        WRITE (6,101) I,NDUM,(X(I,K),K=1,2)
        IF (I-J) 11,10,11
11      WRITE (6,102)
        CALL EXIT
10      CONTINUE
        WRITE (6,106)
        NTDF=3*NJT          $ DO 15 I=1,NTDF      $ DO 15 J=1,NTDF
15      ST(I,J)=0.0
        DO 20 N=1,NEL
        READ (5,101) I,J,  XI,XK
        WRITE (6,101) I,J,XI,XK
        CALL ELEGD (A,XI,XK,E,XMU,I,J)
        IS1=3*(I-1)         $ JS1=3*(J-1)
        DO 20 IK=1,3        $ IS=IS1+IK           $ JS=JS1+IK
        DO 20 JK=1,3        $ ISC=IS1+JK          $ JSC=JS1+JK
        ST(IS,ISC)=ST(IS,ISC)+EKG(IK,JK)
        ST(JS,JSC)=ST(JS,JSC)+EKG(IK+3,JK+3)
        ST(IS,JSC)=ST(IS,JSC)+EKG(IK,JK+3)
20      ST(JSC,IS)=ST(IS,JSC)
        IF (NR.EQ.0) GO TO 14
        DO 13 M=1,NR
        LL=NDR(M)
        DO 12 I=1,NTDF
```

```
      ST(LL,I)=0.0
12    ST(I,LL)=0.0
13    ST(LL,LL)=1.0
14    CONTINUE
      WRITE (6,100)
      DO 26 I=1,NTDF
26    WRITE (6,103) I, (ST(I,J),J=1,NTDF)
      CALL CONDEN (NJT,NTDF,ST)
      STOP                    $ END
      SUBROUTINE ELEGD (A,XI,XK,XE,XMU,L,M)
      COMMON X,DA
      DIMENSION  X( 60,2),DA(6,6),E(6,6),ED(6,6,
      A1=X(M,1)-X(L,1)     $ A2=X(M,2)-X(L,2)
      S=SQRT(A1**2+A2**2) $G1=A1/S                  $ G2=A2/S
C     *** TRANSFORMATION MATRIX (DIRECTION COSINES) ***
      DO 10 I=1,6          $ DO 10 J=1,6
10    DA(I,J)=0.0
      DA(1,1)=1.0          $ DA(2,2)=G1             $ DA(2,3)=G2
      DA(3,2)=-G2          $ DA(3,3)=G1          $ DA(4,4)=1.0
      DA(5,5)=G1           $ DA(5,6)=G2          $  DA(6,5)=-G2
      DA(6,6)=G1
      XG=XE/(2.0*(1.0+XMU))
      C=XE*XI/S**3
C     *** ELEMENT STIFFNESS ***
      E(1,1)=12.0          $ E(2,1)=0.              $ E(3,1)=-6.0*S
      E(4,1)=-12.          $ E(5,1)=0.           $ E(6,1)=-6.0*S
      E(2,2)=XG*XK/S/C     $ E(3,2)=0.
      E(4,2)=0.            $ E(5,2)=-E(2,2)         $ E(6,2)=0.
      E(3,3)=4.*S**2       $ E(4,3)=6.*S            $ E(5,3)=0.
      E(6,3)=2.*S**2       $ E(4,4)=12.             $ E(5,4)=0.
      E(6,4)=6.*S          $ E(5,5)=E(2,2)          $ E(6,5)=0.
      E(6,6)=4.*S**2
      DO 20 I=1,5          $ K=I+1                  $ DO 20 J=K,6
20    E(I,J)=E(J,I)
      DO 30 I=1,6          $ DO 30 J=1,6
30    E(I,J)=C*E(I,J)
C     *** E TIMES DA ***
      DO 40 I=1,6          $ DO 40 J=1,6
      ED(I,J)=0.           $ DO 40 K=1,6
40    ED(I,J)=ED(I,J)+E(I,K)*DA(K,J)
C     *** TRANSPOSE OF TRANSFORMATION MATRIX ***
      DO 50 I=1,6          $ DO 50 J=1,6
50    E(I,J)=DA(J,I)
C     *** MEMBER STIFFNESS IN GLOBAL COORD. ***
      DO 60 I=1,6          $ DO 60 J=1,6
      DA(I,J)=0.           $ DO 60 K=1,6
60    DA(I,J)=DA(I,J)+E(I,K)*ED(K,J)
      RETURN               $ END
      SUBROUTINE CONDEN (NJT,NTDF,A)
      DIMENSION LS(120),A(170,170)
      N=1
      DO 10 M=1,NJT
      DO 10 MJ=2,3
      LS(N)=3*(M-1)+MJ
      N=N+1
```

```
10      CONTINUE
11      FORMAT (1X,I3,1X,10E13.5,/(5X,10E13.5))
12      FORMAT (1H1)
107     FORMAT (1X,* CONDENSED STIFFNESS MATRIX *)
101     FORMAT (I10)
        MM=2*NJT
        WRITE (6,12)
        DO 1 M=1,MM
        WRITE (6,101) M
        L=LS(M)
        II=3
        DO 2 I=1,NTDF,II
        IF ((L-I)-1) 4,5,6
4       II=1
        GO TO 7
5       II=2
        GO TO 7
6       II=3
7       CONTINUE
        JJ=3
        DO 3 J=1,NTDF,JJ
        IF ((L-J)-1) 14,15,16
14      JJ=1
        GO TO 17
15      JJ=2
        GO TO 17
16      JJ=3
17      CONTINUE
        A(I,J)=A(I,J)-A(I,L)*A(J,L)/A(L,L)
3       CONTINUE
2       CONTINUE
1       CONTINUE
        WRITE (6,12)
        WRITE (6,107)
        DO 21 I=1,NJT
        M=3*(I-1)+1
        DO 20 J=1,NJT
        N=3*(J-1)+1
20      A(I,J)=A(M,N)
21      WRITE (6,11) I,(A(I,J),J=1,NJT)
        RETURN      $ END
```

Flow Chart for the Program of Dynamic Response of a Multi-Degree-Freedom System

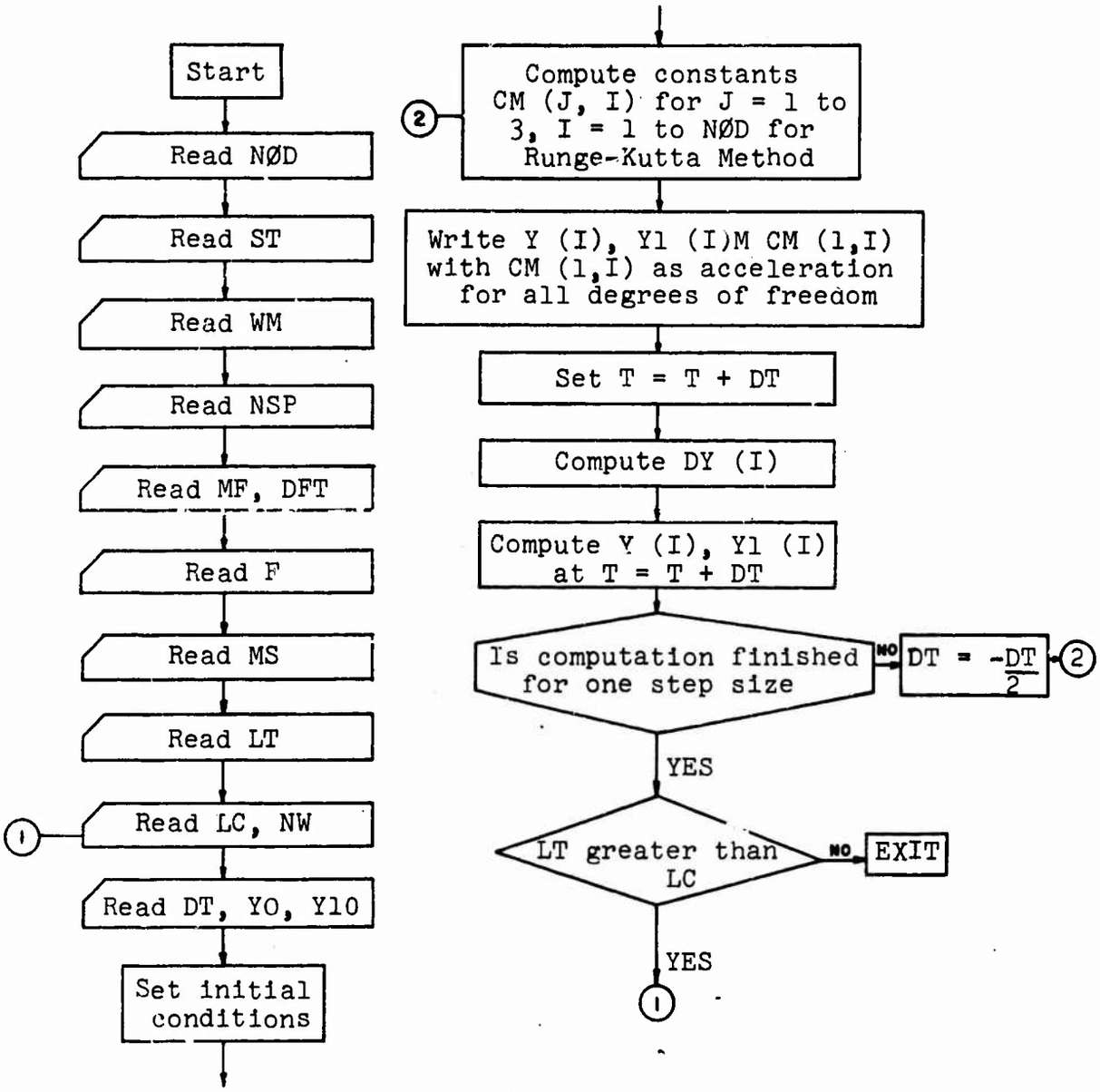

Input Sequence for the Program for Computing the Dynamic Response of a Multi-Degree-Freedom System

1. NØD
   Format (10I8)
   NØD: number of degrees of freedom in system.

2. ST(I,J), J = 1, NØD
   Format (6E13.6)
   ST: elements of stiffness matrix of the system.

3. WM(I), I = 1, NØD
   Format (10F8.5)
   WM: mass corresponding to each degree of freedom, because of the assumption of lumped system.

4. NSP
   Format (10I8)
   NSP: degree of freedom corresponding to the point subjected to the external forces.

5. MF, DFT
   Format (I8, F8.3)
   MF: number of forces
   DFT: time interval
   For example: A continuous forcing function f(t) between $a \leq t \leq b$. If b - a is divided into n parts, then
   $DFT = \frac{b-a}{n}$, MF = n + 1.

6. F(I), I = 1, MF
   Format (10F8.0)
   F = magnitude of force equal to $f(t_i)$ in the example under 5.

7. MS(I), I = 1, NØD.
   Format (10I8)
   In the case the stiffness matrix must be reduced in size, MS(I) indicates the number of degree of freedom of the original matrix retained.
   For example: original matrix has 6 degrees of freedom. If 2, 3 are eliminated, then MS(I) = 1,4,5,6 and the reduced matrix has 4 degrees of freedom ranging from 1 to 4.

8. LT
   Format (10I8)
   In the numerical technique, step size (time increment)

has to be decided. If several step sizes are to be tried during one run, put LT equal to the number of step sizes.

9. LC, NW
Format (10I8)
LC = 1 corresponds to the first step size, LC = 2 corresponds to second step size, etc.
NW: If step size equals DT, the print out of the dynamic response will be in the time interval of (DT) x (NW).

10. DT, YO, Y10
Format (10F8.5)
DT = step size (time increment in calculation)
YO = initial displacement for all degrees of freedom
Y10 = initial velocity for all degrees of freedom.

Note. If initial conditions are different for each degree of freedom, the program and the input data for this information must be modified.

```
C       DYNAMIC RESPONSE OF MULTI-DEGREE-FREEDOM SYSTEM
C       CDC 6600 ,  FORTRAN IV , STORAGE REQUIRED  30000 WORDS
        COMMON F,DFT,DT,MF
        DIMENSION ST(60,60),Y(60),DF(60),CM(3,60),R(60),DY(60),WM(60)
        DIMENSION EY(60),EF(60),Y1(60)
        DIMENSION F(200)
        DIMENSION RY(60),MS(60)
C       FORMAT(1H1) IS TO TELL THE PRINTER TO START A NEW PAGE
 9051   FORMAT (1H1)
  101   FORMAT(   52H  TIME    NODES      DISP.      VELOCITY  ACCELERATION)
102     FORMAT (10F8.5)
  103   FORMAT(4F10.5)
104     FORMAT (9X,2I5,2X,3E12.5)
105     FORMAT (* NOD=*,I3)
  106   FORMAT (  52H  SEC                  IN          IN/SEC  IN/SEC/SEC  )
107     FORMAT (F9.6,2I5,2X,3E12.5)
108     FORMAT (6E13.6)
109     FORMAT (10F8.0)
110     FORMAT (10I8)
111     FORMAT (I8,F8.3)
112     FORMAT (* DT=*,F8.6,* Y0=*,F10.3,* Y10=*,F10.3)
        READ (5,110) NOD
        FNOD=NOD
C       READ THE STIFFNESS MATRIX
        DO 51 I=1,NOD
51      READ (5,108) (ST(I,J),J=1,NOD)
        READ (5,102) (WM(I),I=1,NOD)
        DO 52 I=1,NOD
52      DF(I)=0.0
        READ (5,110) NSP
        DF(NSP)=1.0
        READ (5,111) MF,DFT
        READ (5,109) (F(I),I=1,MF)
        F(MF+1)=F(MF)
        READ (5,110) (MS(I),I=1,NOD)
        WRITE(6,9051)
501     FORMAT (* STIFFNESS MATRIX *)
502     FORMAT (* MASS AND FORCE FACTOR *)
503     FORMAT (* ORIGINAL TIME INTERVAL AND EXTERNAL FORCE *)
601     FORMAT (I3,I3,10F10.0/ (6X,10F10.0))
602     FORMAT (I3,2X,2F10.5)
603     FORMAT (2X,* NO. FORCE =*,I3,* TIME INTERVAL =*,F5.3)
604     FORMAT (10F10.0)
        WRITE (6,105) NOD
        WRITE (6,501)
        DO 60 I=1,NOD
60      WRITE (6,601) MS(I),I,(ST(I,J),J=1,NOD)
        WRITE (6,502)
        WRITE (6,602) (I,WM(I),DF(I),I=1,NOD)
        WRITE (6,503)
        WRITE (6,603) MF,DFT
        WRITE (6,604) (F(I),I=1,MF)
        WRITE (6,9051)
        READ (5,110) LT
30      CONTINUE
```

```
      READ (5,110) LC,NW
      READ(5,102) DT,YO,Y10
      WRITE (6,112) DT,YO,Y10
      XMF=MF
      NF=DFT*XMF/DT+0.5
      WRITE(6,101)
      WRITE(6,106)
      DO 1 I=1,NOD
      Y(I)=YO
    1 Y1(I)=Y10
      IT=1
      T=0.
      NI=0
    2 ET=-DT/2.
      DFF=(FF(IT+1)-FF(IT))/2.0
      DO 8 I=1,NOD
    8 EY(I)=Y(I)-DT/2.*Y1(I)
C     J (EQUAL TO 1, 2, 3, ) IS THE SUBSCRIPT  FOR COMPUTING THE
C     CONSTANTS M,S IN THE NUMERICAL INTEGRATION PROCEDURE
      DO 4 J=1,3
      AA=J-1
      ET=ET+DT/2.
      FT=FF(IT)+DFF*AA
      DO 9 I=1,NOD
      EY(I)=EY(I)+DT/2.*Y1(I)
9     EF(I)=FT*DF(I)
C     SUBROUTINE RR IS TO COMPUTE THE RESISTING FORCES AT THE
C     PIVOTAL POINTS
      CALL RR(R,ST,EY,NOD)
      DO 4 I=1,NOD
    4 CM(J,I)=Y2F(EF(I),R(I),WM(I))
      NIT=NW*NI+1
      IF (NIT.NE.IT) GO TO 22
      NI=NI+1
      DO 21 I=1,NOD
      IF (I.EQ.1)WRITE(6,107)T,MS(I),I,Y(I),Y1(I),CM(1,I)
      IF(I.NE.1)WRITE(6,104) MS(I),I,Y(I),Y1(I),CM(1,I)
   21 CONTINUE
22    CONTINUE
      T=T+DT
      IT=IT+1
      DO 6 I=1,NOD
      DY(I)=Y1(I)*DT+DT/6.*(CM(1,I)+2.*CM(2,I)) *DT
      Y1(I)=Y1(I)+DT/6.*(CM(1,I)+4.*CM(2,I)+CM(3,I))
      Y(I)=Y(I)+DY(I)
      IF (Y(I).LT.0.) CALL EXIT
6     CONTINUE
      IF (NF.GT.IT) GO TO 2
      IF (LT.GT.LC) GO TO 30
      STOP      $ END
      SUBROUTINE RR(R,ST,Y,NOD)
      DIMENSION R(60),ST(60,60),Y(60)
      DO 3 I=1,NOD
      R(I)=0.
      DO 3 J=1,NOD
```

```
    3 R(I)=R(I)+ST(I,J)*Y(J)
      RETURN
      END
      FUNCTION Y2F(EF,R,WM)
      G=386.2
1     Y2F=(WM*G-EF-R)/WM
2     RETURN
      END
      FUNCTION FF(IT)
      DIMENSION F(200)
      COMMON F,DFT,DT,MF
      X=DFT/DT
      XIT=IT
      N=XIT/X
      IF (N.LT.0) N=1
      DO 1 I=N,MF
      XI=I
      XNI=(XI-1.)*X
      IF (XIT.LT.XNI) GO TO 2
1     CONTINUE
2     Y=-(XNI-XIT)+X-1.
      A=F(I)
      B=F(I-1)
      C=(A-B)/X
      FF=B+C*Y
      RETURN    $    END
```

UNCLASSIFIED
Security Classification

DOCUMENT CONTROL DATA - R & D

(Security classification of title, body of abstract and indexing annotation must be entered when the overall report is classified)

1. ORIGINATING ACTIVITY (Corporate author)
University of Texas at Austin
Austin, Texas

2a. REPORT SECURITY CLASSIFICATION
UNCLASSIFIED

2b. GROUP

3. REPORT TITLE
Stress and Deflections in Type II and Type IV Airdrop Platforms.

4. DESCRIPTIVE NOTES (Type of report and inclusive dates)
Final Report

5. AUTHOR(S) (First name, middle initial, last name)
Wen Shing Chang
E. A. Ripperger

6. REPORT DATE	7a. TOTAL NO. OF PAGES	7b. NO. OF REFS
December 1969	79	7

8a. CONTRACT OR GRANT NO.	9a. ORIGINATOR'S REPORT NUMBER(S)
DAAG 17-67-C-0189	
b. PROJECT NO.	
c. 1M121401D195	9b. OTHER REPORT NO(S) (Any other numbers that may be assigned this report)
d.	70-56-AD

10. DISTRIBUTION STATEMENT
This document has been approved for public release and sale; its distribution is unlimited.

11. SUPPLEMENTARY NOTES	12. SPONSORING MILITARY ACTIVITY
	US Army Natick Laboratories Natick, Massachusetts 01760

13. ABSTRACT

Severe stress conditions may develop during the extraction and parachute deployment phases of an airdrop with a stressed platform. The platform stresses and deflections during that dynamic loading period are computed by treating the platform as a planar network of beams rigidly connected at the joints. Stiffness properties of the beams in the network are calculated approximately using standard methods and then refined to more exact values by comparing measured deflections under static loading to computed deflections. These stiffness properties are then used in the analysis of the dynamic load. Equations of motion are written for each degree of freedom using a lumped mass representation for the loads. Deflections at the joints of the network are obtained by solving the equations of motion using the Runge-Kurt-Gill numerical procedure. Stresses are then determined from the deflections. It is found that the maximum deflection at the center of a 3 module, Type II platform loaded with a total load of 9000 lb distributed over the central portion of the platform is 5.17 in. dynamically, as compared to 1.89 in. for static loading. The maximum stress at the center of the platform is 24,500 psi for the dynamic loading as compared to 6230 psi for static loading. Similar results for the Type IV platform are not available. Also, dynamic stresses in the side rails have not been completed.

DD FORM 1 NOV 68 1473 REPLACES DD FORM 1473, 1 JAN 64, WHICH IS OBSOLETE FOR ARMY USE.

UNCLASSIFIED
Security Classification

14. KEY WORDS	LINK A		LINK B		LINK C	
	ROLE	WT	ROLE	WT	ROLE	WT
Stresses	8					
Deflection	8					
Platforms	9					
Deployment	10					
Parachutes	10					
Aerial Delivery	4					